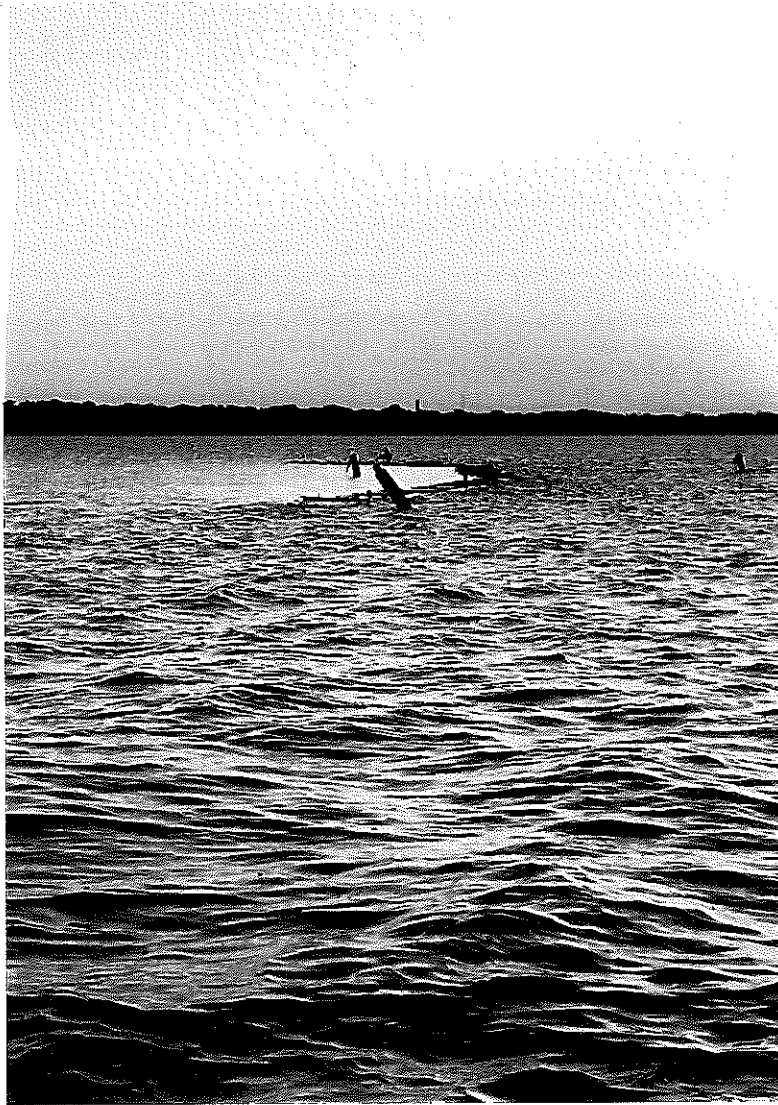


Lake Thunderbird Shoreline Erosion Research Project

Final Project Report



Submitted by:

School of Civil Engineering and Environmental Science
University of Oklahoma

Submitted to:

Central Oklahoma Master Conservancy District

September 2021

Contents	
List of Figures	4
List of Tables	5
Executive Summary	7
1 Objectives	8
2 Literature Review	9
2.1 Shoreline Erosion	10
2.2 Lake Thunderbird	11
2.3 Breakwaters	12
2.3.1 Bottom-Mounted Breakwaters	12
2.3.2 Floating Breakwaters	13
2.4 Floating Treatment Wetlands	18
2.5 Floating Wetland Breakwaters	19
2.6 Similitude	20
3 Methods	21
3.1 Full-scale Controlled Mesocosm	21
3.1.1 Experimental Setup	22
3.1.2 Wave Height Data Collection	27
3.2 Laboratory-scale Controlled Scale Models	28
3.2.1 Scaling	29
3.2.2 Experimental Setup	32
3.2.3 Wave Height Data Collection	33
3.3 Field-scale Implementation and Monitoring	33
3.3.1 Wave Height Data Collection	35
3.3.2 Biological Sampling	36
3.3.3 Jet Erosion Test	37
3.3.4 Estimation of Wave Energy to Cause Erosion	37
4 Results and Discussion	39
4.1 Full-scale Controlled Mesocosm	40
4.1.1 Wave Height	40
4.1.2 Wave Energy Density	41
4.1.3 Preliminary Cost Analysis	42
4.2 Laboratory-scale Controlled Scale Models	43

4.2.1. Wave Height and Energy Reduction	43
4.3 Field-scale Implementation	48
4.3.1 Wave Height and Energy Reduction	48
4.3.2 Estimation of Long-term Erosion Minimization at the Study Bank	50
4.3.2.1 Jet Erosion Test (JET) Results	50
4.3.2.2 Comparison to Long-term Estimated Wave Heights	52
4.4 Discussion Comparing All Three Scales	54
4.4.1 Wave Transmission Coefficient Comparison	54
4.4.2 Comparisons of the Implemented Design at Three Scales	56
4.5 Opportunistic Biological Monitoring	57
4.5.1 Fish Surveys	57
4.5.2 Plant Monitoring	60
4.6 Cost Analysis Comparison to Other Best Management Practices	61
5 Lessons Learned and Design Alterations	62
6 Recommendations for Future Work	66
6.1 Media and Plant Establishment	66
6.2 One-piece Frame	68
6.3 Wave Measurement	69
7 Summary and Conclusions	69
References	70

List of Figures

Figure 1: Types of bottom-mounted breakwaters (Environmental Protection Agency, 2006)	13
Figure 2. Schematics of two types of box breakwaters (McCartney, 1985).	15
Figure 3. Schematic of four types of pontoon breakwaters (McCartney, 1985).	16
Figure 4. Schematic to two types of mat breakwater systems	16
Figure 5. Schematics of two types of tethered float breakwater systems (McCartney, 1985).	17
Figure 6. Side view of a Y-frame floating breakwater (McCartney, 1985).	18
Figure 7. Aerial view of the Aquatic Research Facility study pond location in Norman, Oklahoma.	22
Figure 8. Cross-sectional view of the prototype floating wetland breakwaters showing the dimensions of the pipe ballasts.	23
Figure 9. Top view of the prototype floating wetland breakwater frame, showing the top dimensions in inches.	23
Figure 10. Three-dimensional representation of the FWB design shown from underneath (top) and above (bottom).	24
Figure 11. Floating wetland breakwater frame used for the prototype system (upside-down). Photo by Maxwell O'Brien.	25
Figure 12. Custom wave generator used for the prototype system. Photo by Maxwell O'Brien.	27
Figure 13. Experimental setup for the full-scale mesocosm system at the Aquatic Research Facility in Norman, Oklahoma.	28
Figure 14. Calculations for the number of pipes for the floating wetland breakwater scale models.	30
Figure 15. Calculations of the errors resulting from the difference in numbers of pipes for the floating wetland breakwater scale models.	30
Figure 16. Experimental setup for the scale model similitude studies in Carson Engineering Center at the University of Oklahoma.	33
Figure 17. Location of field implementation for the 200-ft floating wetland breakwater. The study location is highlighted by the red rectangle.	34
Figure 18. Diagram of the design of the 200-ft section of floating wetland breakwater installed into Lake Thunderbird, including anchors and buoys.	35
Figure 19. Incoming and outgoing wave height comparisons and linear trendlines for the full-scale mesocosm at the Aquatic Research Facility at the University of Oklahoma in Norman, Oklahoma.	40
Figure 20. Incoming and outgoing wave energy density comparisons and linear trendlines for the full-scale mesocosm at the Aquatic Research Facility at the University of Oklahoma in Norman, Oklahoma.	41
Figure 21. Front and back average wave height comparisons for the full-scale and 1:8 scale for (A) no pipe design, (B) 11 pipes, 1 foot long design, (C) 6 pipes, two foot long, (D) 11 pipes, 2 foot long, and (E) 11 pipes, 3 foot long.	44
Figure 22. Front and back average wave energy density comparisons for the full-scale and 1:8 scale for (A) no pipe design, (B) 11 pipes, 1 foot long design, (C) 6 pipes, two foot long, (D) 11 pipes, 2 foot long, and (E) 11 pipes, 3 foot long.	45
Figure 23. Comparison of the average critical wave height before and after a wave crosses the floating wetland breakwaters installed at Lake Thunderbird.	49
Figure 24. Comparison of the average wave energy density before and after a wave crosses the floating wetland breakwaters installed in Lake Thunderbird.	49
Figure 25. Jet erosion test (JET) comparison graph showing the observed values collected in the field to the three JET solutions.	51

Figure 26. Histogram showing the historical wind speed and the frequency each one occurred for winds from the Southeast to Southwest. (Source: Norman, Oklahoma Mesonet Site).....	53
Figure 27. Comparison of wave reduction caused by floating wetland breakwaters for all three scales of this study for the implemented design [full-scale mesocosm (blue), laboratory scale (red), and field (yellow)], which had 11 ballast pipes that were 3 feet long.	56
Figure 28. Comparison of wave energy density reduction caused by floating wetland breakwaters for all three scales of this study for the implemented design [full-scale mesocosm (blue), laboratory scale (red), and field (yellow)], which had 11 ballast pipes that were 3 feet long on each 10-foot section.....	57
Figure 29. Average Greenseeker normalized difference vegetation index (NDVI) values measured at a constant height above floating wetland breakwater frames in September and October 2020.....	60
Figure 30. Evolution of floating wetland media design from initial planting and installation (left) to the damaged wetland frames (center), to finally the design modifications (right) to make the Polyflo more stable in the frames.....	63
Figure 31. Coir mattress production process.....	64
Figure 32. Demonstration of situating and planting the coir mattresses in the frame (top row), along with the frames positioned in the water (bottom image). Photos taken by Maxwell O'Brien.	65
Figure 33. Top view (top) of the cross-brace modifications (blue) made to the original floating wetland breakwater design. Cross braces seen being attached to the floating wetland breakwater fram in the bottom image. Photo taken by Maxwell O'Brien.....	66
Figure 34. Roots from <i>Juncus Effusus</i> growing through PolyFlo media prior to field deployment in 2020.....	68

List of Tables

Table 1. Incremental pollutant removal rates for floating treatment wetlands in ponds (Scheuler et al., 2016).	19
Table 2. Wave energy density comparisons for various floating wetland breakwater frame designs for a six inch wave. Design configurations show the number and length of pipe ballasts. ** the six pipe, three foot tests represented a limited range of wave height.	41
Table 3. Preliminary cost analysis based on price per 10-ft length of material and the corresponding amounts of wave energy density reduction, based on a six-inch wave. The bolded selection indicates the design that was selected for field implementation.	42
Table 4. p values for Mann-Whitney U test comparing prototype scale and 1:8 model scale wave height and wave-energy density distributions for different floating wetland breakwater frame ballast configurations.....	46
Table 5. p values from Mann-Whitney U test comparing wave height reduction of different floating wetland breakwater (FWB) configurations at the laboratory 1:8 model scale. p values less than 0.05 are highlighted and are considered significantly different.	47
Table 6. p values from Mann-Whitney U test comparing wave energy density reduction of different floating wetland breakwater (FWB) configurations at the laboratory 1:8 model scale. p values less than 0.05 are highlighted and are considered significantly different.	47
Table 7. p values from Mann-Whitney U test comparing wave height reduction of different floating wetland breakwater (FWB) configurations for the full-scale mesocosm. p values less than 0.05 are highlighted and are considered significantly different.	48

Table 8. p values from Mann-Whitney U test comparing wave energy density reduction of different FWB skirt wall configurations for the full-scale mesocosm. p values less than 0.05 are highlighted and are considered significantly different.....	48
Table 9. Percentage of waves in various height ranges with and without floating wetland breakwaters, based on wave height estimations for 5-minute wind speeds from the Norman, Oklahoma Mesonet site (https://www.mesonet.org/index.php/sites/site_description/nrmn).....	54
Table 10. Range of wave transmission coefficient values (K_t) for floating breakwaters on other studies and the floating wetland breakwater designs investigated in this study.....	55
Table 11. Fish survey results from the floating wetland breakwater and control site, completed in November 2019.....	59
Table 12. Fish survey results from the floating wetland breakwater and control site, completed in August 2020.....	59
Table 13. Comparison of one-time materials cost and cost per day for no erosion over an assumed 20-year design life for various best management practices. These calculations do not consider inflation.	61

Executive Summary

Lake Thunderbird, which is located to the east and south of Oklahoma City, is on the Army Corps of Engineers 303(d) list of impaired water bodies due to three limiting factors, one of which is turbidity. The lake has approximately 50 miles of shoreline with 83% having some degree of erosion. Over the years, shoreline erosion has resulted in significant loss of shoreline and deposition of the eroded material into the lake, effectively reducing the holding capacity of the lake and adversely affecting water quality. To reduce the erosive action of the waves, this project completed to utilize floating wetland breakwaters (FWBs) anchored near the shoreline to reduce the energy from wave action.

The three objectives of this study were: (1) Test multiple FWB frame designs to determine the best design for maximizing wave-energy reduction; (2) Complete laboratory-scale experiments on model FWB frames to determine the viability of using scale models to predict full-scale performance; and (3) Complete field testing of the selected design to determine in-situ wave reduction and the resulting impact on shoreline erosion.

Overall, the project was successful in meeting the three project objectives. The full-scale mesocosm demonstrated that a frame design with 11 ballasts that were each 3-feet long per 10-foot section provided the most wave energy reduction per materials cost. Through the laboratory-scale experiments, we were able to utilize similitude concepts to demonstrate that, in general, we were able to predict full-scale wave-reduction performance using smaller scale models when similitude concepts are recognized in the design. Finally, our field implementation resulted in the best wave reduction performance of all of our tests at multiple scales, including comparisons to designs available in literature. Based on wind speed and fetch data for southerly

winds and shear stress determination from the shoreline soils, we estimate that our FWB design is able to reduce 96% of the waves to height smaller than what is required to cause detachment erosion on that bank. In addition, the materials cost per foot was comparable to other shoreline erosion techniques. Within this report, we also discuss lessons learned during our process, along with next steps for further development of this FWB concept.

1 Objectives

Lakes and reservoirs are subject to water waves due to wind and wake action. These waves transfer energy that erodes and transports bank soil. This erosion affects ecosystems by reducing viable habitat on shorelines and banks, decreasing species diversity, and impacting water quality within the reservoir. As a result, there is a need for ways to reduce wave action in water bodies before they reach the shoreline. Floating breakwaters have been used to reduce wave size and floating wetlands have mostly been used to provide habitat and improve water quality. Using floating wetlands as breakwaters grants the benefits from both systems. The goal of this project is to determine the best design for FWBs for minimizing wave energy which will cause detachment erosion on reservoir shorelines. Overall, it is expected that these results will be best applied to shorelines with moderate erosion, as opposed to extreme erosion areas with a cut bank where mass wasting will be the dominant form of erosion.

The three objectives of this study were: (1) Test multiple FWB frame designs to determine the best design for maximizing wave energy reduction; (2) Complete laboratory-scale experiments on model FWB frames to determine the viability of using scale models to predict full-scale performance; and (3) Complete field testing of the selected design to determine in-situ wave reduction and the resulting impact on shoreline erosion. These objectives were addressed

through the following tasks: (1) Complete a literature review on floating breakwaters and floating wetlands; (2) develop a range of FWB frame designs and test them in a full-scale mesocosm with controlled, artificial waves; (3) test scaled-down versions of the FWB to investigate similitude relationships and the ability to use small-scale models to predict performance at full scale; (4) install and monitor wave reduction for the best design at one location in Lake Thunderbird; (5) use a jet erosion test (JET) to determine the critical shear stress and resulting wave height required for detachment erosion to occur at the bank of interest; (6) utilize the monitoring and JET results to predict long-term wave a reduction at the Lake Thunderbird site based on soil type and historical wind data; (7) opportunistically collect other relevant data and observations, which may include fish population, plant root length, media type integrity, and plant coverage in the design implemented in the reservoir, and (8) discuss lessons learned and future recommendations for continued design and implementation improvements.

Overall, there is a gap in current research on the design and use of floating wetlands as wavebreaks. A broad body of knowledge on wavebreaks is present in both coastal and inland water settings. Floating wetlands have utilized for water quality and habitat improvement. However, floating wetlands have generally not been designed with wave reduction as the primary objective. A FWB has the potential for wave reduction while also providing other ecosystem benefits. Additionally, investigation of the similitude relationships associated with their performance allows for efficient design and implementation at multiple scales and in different sizes of reservoirs.

2 Literature Review

Coastal systems, lakes and reservoirs are subject to shoreline erosion. Breakwaters have been utilized in these systems for wave reduction, and floating wetlands have been utilized for water quality and habitat improvements. FWBs can potentially be used to provide all of these benefits. Performing a similitude study on FWBs can determine how they would perform when designed for different scales. Furthermore, implementation and monitoring of a FWB in a reservoir, such as Lake Thunderbird, can provide insight and direction of how to best implement these structures for shoreline erosion management.

2.1 Shoreline Erosion

Erosion is the geological process in which earthen materials are worn away and transported by natural forces such as wind or water (National Geographic Society, 2018). While this process occurs across the landscape, shoreline erosion has been a serious concern in reservoirs around the world. Shoreline erosion can occur by two principle mechanisms— detachment erosion, which is the dislodging of the soil particle from water impact, and mass wasting, which is the movement of rock and soil down a slope under the influence of gravity. This study will focus on wave reduction, which is a primary cause of detachment erosion on shorelines.

Marani et al. (2011) used observations and dimensional analysis to determine that the erosion rate of marsh edges was directly proportional to wave power. Leonardi et al. (2016) used data from eight different sites in the United States, Italy, and Australia, and found a linear positive relationship between wave power and erosion rate in salt marshes. Ozeren and Wren (2018) performed a wave erosion analysis on cohesive and non-cohesive embankments and concluded that both embankments eroded at a similar rate due to wave action. Water waves are often a function of the wind speed and direction (Kinsman, 2002; Sayah et al., 2005). In large

reservoirs, there is enough space for wind to gradually form bigger waves that hit the shore with relatively high energy. This accentuates the erosion process of the shore. For natural systems that are not heavily destabilized, reducing the forcing function of the waves can reduce the erosion of the shoreline.

The negative effects of shoreline erosion on local ecosystems include loss of property, water quality issues from the soils eroding into the lake, loss of shoreline access for recreation, and habitat destruction for fisheries and wildlife (Allen, 2001). Sadeghian et al. (2017) states that the accumulation of sediment in a reservoir decreases the storage capacity and lifespan of the reservoir.

2.2 Lake Thunderbird

Lake Thunderbird is a 6,070-acre reservoir in northeast Cleveland County, Oklahoma, that impounds the Little River and Hog Creek, and has approximately 86 miles of shoreline (Wu et al., 2019). It has a long history of sediment impairment and is currently on the EPA 303(d) list for impairment by turbidity, which is caused by excess sediment both from erosion from within the watershed and from the shoreline or the reservoir (ODEQ, 2020). Allen (2001) describes the shoreline of the lake as variations of red sandy clay loams that are underlain by sandstone and shale. Furthermore, they describe the soils “very noncohesive, nutrient deficient, and tend to be acidic. These characteristics together make these soils very erosive and difficult to revegetate without man’s assistance.” A bathymetric study of the lake conducted by the OWRB (2002) found that the pool capacity of the lake has been reduced from 119,600 acre-feet in 1966 to 105,644 acre-feet in 2001 for a loss of capacity of 13,956 acre-feet or 11.7% in 35 years (OWRB, 2002). This observed loss rate is 14% higher than reportedly estimated by the United States Bureau of Reclamation in correspondence with the OWRB in 1965, which was attributed

to “larger grained sediment washed in from the watershed” (OWRB 2002). Wu et al. (2019) has also recommended that best management practices (BMPs) be adopted to prevent shoreline erosion.

2.3 Breakwaters

2.3.1 Bottom-Mounted Breakwaters

Breakwaters are structures that have been widely used to dissipate wave energy and protect shorelines. They are common in harbors and come in different forms. The main types of bottom-mounted breakwaters are: conventional rubble mound breakwater, rubble mound breakwater with monolithic crown wall, berm or S-slope breakwater and caisson-type breakwater (EPA, 2006). These breakwater designs are shown in Figure 1. Conventional rubble mound breakwaters have a trapezoidal cross section with an armour layer and are preferred in locations where the water depth is less than 15 m because of the amount and cost of material required for construction. Conventional rubble mound breakwaters with crown walls are mainly used for port protection and allow access to the breakwater for port operations and maintenance. For berm breakwaters, the armourstone is placed in a berm on the seaward slope. The armourstone, the rock used for wave protection, is allowed to move to a certain extent during severe storm events to form a stable profile. Low-crested breakwaters are used for protection in areas where overtopping is acceptable. They are usually built when aesthetics are considered and can be partially emergent or fully submerged. Caisson-type breakwaters are rubble-mound breakwaters with a caisson on top of the mound. These are mainly used for port protection and are less expensive than conventional rubble mound breakwaters in water depths above 15-m. Finally, horizontally composite breakwaters are rubble-mound breakwaters with a caisson behind the mound. These types of breakwaters are built on the seafloor and may be connected to

the shore. Bottom-mounted breakwaters require relatively large quantities of material and are often not aesthetically pleasing. As a result, these types of breakwaters are mainly used in ports and harbors where the safety of local workers is of great concern.

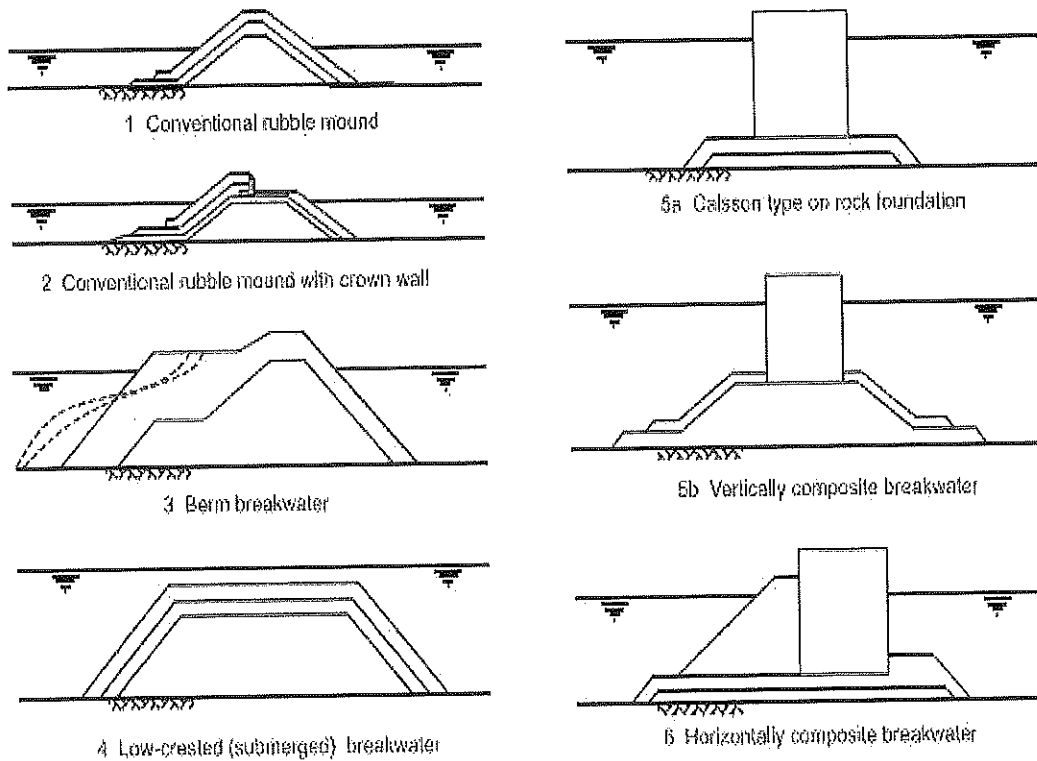


Figure 1: Types of bottom-mounted breakwaters (Environmental Protection Agency, 2006)

2.3.2 Floating Breakwaters

Floating breakwaters are floating structures designed to absorb waves and reduce their energy. Floating breakwaters are often restricted to relatively calm and shallow water areas, as they are structurally weaker than bottom-mounted breakwaters (Uzaki et al., 2011). The advantage of floating breakwaters is that they are adaptable to fluctuations in water level, are mobile and easily relocated, are independent of the condition of bottom sediment, and offer less

obstruction to water circulation and fish movement. One drawback of using floating breakwaters is that they offer minimal habitat or water quality improvements. Floating breakwaters are often constructed using concrete or steel and do not provide services to the ecosystem they are in, other than wave reduction.

Structurally, floating breakwaters provide several different advantages compared to traditional fixed breakwater systems. Traditional fixed breakwater systems are usually very difficult and time consuming to install in because they are typically fixed to the water body floor. Floating breakwaters provide an “economic alternative to fixed structures for use in deeper waters,” defined as depths greater than 20 feet (McCartney, 1985). Additionally, floating breakwaters do not disturb or impede aquatic ecosystems, water currents, and fish migrations, nearly as much as traditional fixed breakwaters, therefore preserving wildlife habitats (McCartney, 1985). Further, floating breakwaters do not disturb the underlying sediment as much as traditional fixed break water systems. They also have many potential applications beyond decreasing shoreline erosion, including boat basin protection and boat ramp protection (McCartney, 1985). Floating breakwaters can typically be classified into four different categories, each with their own advantages and disadvantages, which include box, pontoon, mat, and tethered floats.

Box breakwaters (Figure 2) are typically modular and reinforced. Flexible connections between each unit allow the system to act like one entity. These large units are often constructed using concrete or steel (McCartney, 1985). The largest concern for this type of floating breakwaters is the primary points of connection between the other units and the mooring system. The connection points in the modular design can face a significant amount of pressure, causing them to break, which is why they are a major concern. The mooring system is a primary concern

because if the frames become detached from one another the system stops acting as one and loses much of its functionality.



<p><u>BOX</u> Solid rectangle</p>	 <p style="text-align: center;"><u>SECTION</u></p>	<p>Reinforced concrete units are the most common type. They may be empty or filled with light material</p>
<p>Barge</p>	 <p style="text-align: center;"><u>SECTION</u></p>	<p>Derived from army</p>

Figure 2. Schematics of two types of box breakwaters (McCartney, 1985).

Pontoon floating breakwaters (Figure 3) function very similarly to box breakwaters in the sense that they are constructed units positioned in series and connected to each other to function as one. One distinct advantage that pontoon breakwaters have over box breakwaters is that, “the overall width can be of the order of half the wavelength,” making the expected reduction of the wave height significant (McCartney, 1985). The reduction of wave height can be contributed to the total amount of area that the wave has to crest over and cross through before moving on past the breakwater. The disadvantages are similar to those of box floating breakwaters. Uzaki et al. (2011) used a pontoon floating breakwater with a truss in their analysis and found wave transmission coefficients (the ratio of transmitted wave height to the incident wave height) ranging from 0.1 to 1.0, depending on the ratio of water depth to wavelength.

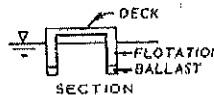
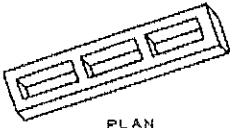
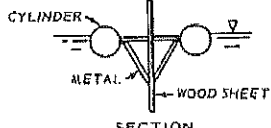

PONTOON Twin pontoon	 SECTION	Calamaran shape
Open compartment	 PLAN	Sometime called Alaska type
A frame	 SECTION	
Twin log	 SECTION	Deck is open wood frame

Figure 3. Schematic of four types of pontoon breakwaters (McCartney, 1985).

Tire-mat breakwaters (Figure 4) are floating mats comprised of new or used tires tied together to form a floating breakwater. These systems have a few distinct advantages including low capital cost, easy removal for maintenance, lower maintenance cost, and low anchors loads required to keep the system in place. However, tire-mat breakwaters also have limited application because they are best suited for areas with mild wave action and can break apart easily, which makes them an environmental liability.



MAT Tire mat	 SECTION	Scrap tires strung on pole framework or bound together with chain or belting. Foam flotation is usually need
Log mat	 PLAN	Log raft chained or cabled together

Figure 4. Schematic to two types of mat breakwater systems.

Tethered float breakwaters (Figure 5) have minimal research on their applicability and effectiveness at reducing incoming wave energy relative to other types of floating breakwaters. Harms (1979) found that tire breakwaters were significantly less expensive than tethered float breakwaters and were also much better at dissipating wave energy.

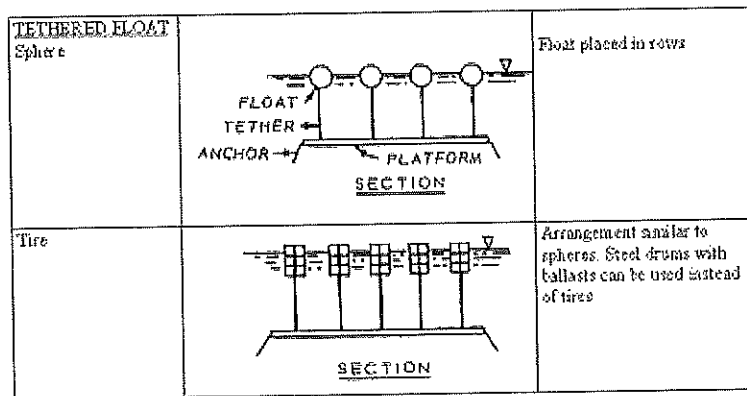


Figure 5. Schematics of two types of tethered float breakwater systems (McCartney, 1985).

The Y-frame floating breakwater includes a ballast or skirt wall attached to the bottom (example shown in Figure 6). Y-frame breakwaters function with ballasts or skirt walls to reduce the breakwater width to wavelength ratio, achieving a lower transmission coefficient, which is the ratio of the power of the incoming to outgoing waves hitting the wavebreak (Mani, 1991; Mani, 2017; Neelamani, 2018). Adding the ballasts thus brings down the capital cost of the system.

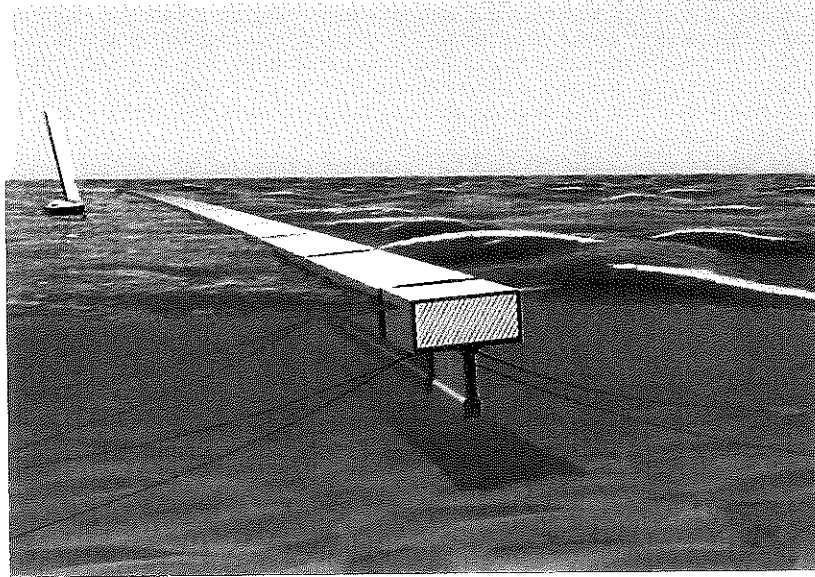


Figure 6. Side view of a Y-frame floating breakwater (McCartney, 1985).

2.4 Floating Treatment Wetlands

Floating treatment wetlands are an emerging engineering option with promise for simultaneous water quality improvement and habitat creation (Strosnider et al., 2017). They are general comprised of rafts that have rooted, emergent macrophytes growing on a mat floating on the surface of the water rather than rooted in the sediment (Headley, 2008). These systems are often engineered to mimic properties of natural floating treatment wetlands, which employ plants and other microbes to take place in phytoremediation, bioremediation, and hydroponics to remove nutrients such as nitrogen and phosphorus. The primary mechanisms that floating treatment wetlands use for nutrient removal are microbial transformation and uptake, macrophyte assimilation, absorption into organic and inorganic substrate materials, and volatilization” (Stewart, 2008). OWRB (2013) demonstrated that floating treatment wetlands are capable of providing water quality and habitat benefits in Lake Eucha in northeast Oklahoma. It has been observed that percent nutrient removal in floating treatment wetlands is directly related

to the percent vegetative coverage of the floating wetland within a water body (Table 1), with a large surface coverage required for significant percent removal of nutrients and total suspended solids (Scheuler et al., 2016). Although full-scale implementation and testing of floating treatment wetlands is limited, they have thus far shown mixed results in improving water quality (Strosnider et al., 2017).

Table 1. Incremental pollutant removal rates for floating treatment wetlands in ponds (Scheuler et al., 2016).

	Raft Coverage in Pond (%)				
	10	20	30	40	50
	Percent Removal (%)				
Total Nitrogen	0.8	1.7	2.5	3.3	4.1
Total Phosphorus	1.6	3.0	4.9	6.5	8.0
Total Suspended Solids	2.3	4.7	7.0	9.0	11.5

2.5 Floating Wetland Breakwaters

Floating wetlands have been shown to be effective for improving water quality and increasing wildlife habitat in a reservoir in Oklahoma (OWRB, 2013). This report also recommended additional research be completed to investigate their potential as wavebreaks to protect the shoreline and reduce overall erosion. In systems where wave reduction is necessary, but aesthetics and ecosystem services are also of concern, a floating wetland breakwater (FWB) hybrid could be a useful solution. However, they must be structural sound enough to withstand the repetitive forces of large waves. Martin Ecosystems (2017) has developed the only commercial application of a floating wetland design that would also work as a breakwater, which has a materials cost of approximately \$270 per foot (Biohaven quote, 2019). Webb (2014) tested the performance of the Martin Ecosystems BioHaven® Floating Breakwater in a controlled flume without plants, with wave transmission coefficients (k_t) ranging between 0.44

and 0.99. This study is the only available literature that the authors could find on the ability of floating wetlands to be utilized primarily as breakwaters.

2.6 Similitude

The concept of similitude is often used so that measurements made on a system at one scale, in the laboratory for example, can be used to describe the behavior of other similar systems outside the laboratory at a larger scale. In engineering, a model is a representation of a physical system that may be used to predict the behavior of the system in some desired respect. The physical system for which the predictions are to be made is called the prototype. With the successful development of a valid model, it is possible to predict the behavior of the prototype under a certain set of conditions. Construction of a successful model is accompanied by an analysis of the conditions it is tested under. Similitude is achieved when there is geometric, kinematic and dynamic similarity between the model and the prototype. A model and prototype are geometrically similar if they are the same shape and all body dimensions in all three coordinates have the same linear-scale ratios. For kinematic similarity, the time rate of change motions of the fluid flow must be the same in the model and the prototype. Dynamic similarity is reached when all the forces acting on the system are in a constant ratio for both scales. Flow conditions for a model test are completely similar if all relevant dimensionless parameters have the same corresponding values for model and prototype. Complete similitude is often not possible; therefore, scaling is usually implemented using the most important dimensionless parameter (Stern, 2013). For systems involving free-surface flow such as flow around a ship or across FWBs, the Froude number is the important similarity parameter. The Froude number is a dimensionless number defined as the ratio of inertial forces to gravitational forces. For free surface flow systems, similitude can be conducted based on an equality of Froude numbers.

Ozeren (2009) and Webb (2014) performed similitude study on floating breakwaters using this method and was able to estimate the wave reduction of a specific floating breakwater design.

3 Methods

To fully understand the capabilities of FWBs for wave reduction, the performance of FWB frame designs were tested at three different scales under artificial and natural conditions. The scales included a full-scale controlled mesocosm, laboratory-scale, and field-scale implementations.

3.1 Full-scale Controlled Mesocosm

A full-scale, controlled mesocosm study was completed to assess the applicability of using floating wetlands as wavebreaks with the goal of reducing bank erosion in reservoirs due to wave action and to determine which design would be best for field implementation into Lake Thunderbird. Prior to field implementation a variety of frame parameters, which will be discussed later, a variety of prototype floating wetland breakwater frames were tested at the Aquatic Research Facility (ARF) of the University of Oklahoma. The ARF is an eight-acre facility located on the south research campus of the university and contains approximately 33 ponds accompanied by four climate-controlled greenhouses. A pond that is 191 feet in length, 48 feet wide, and holds a consistent depth between 5 and 10 feet, seen in Figure 7, was constructed to test the parameter combinations under a variety of wave heights and frequencies to determine which set provided the greatest overall wave reduction.

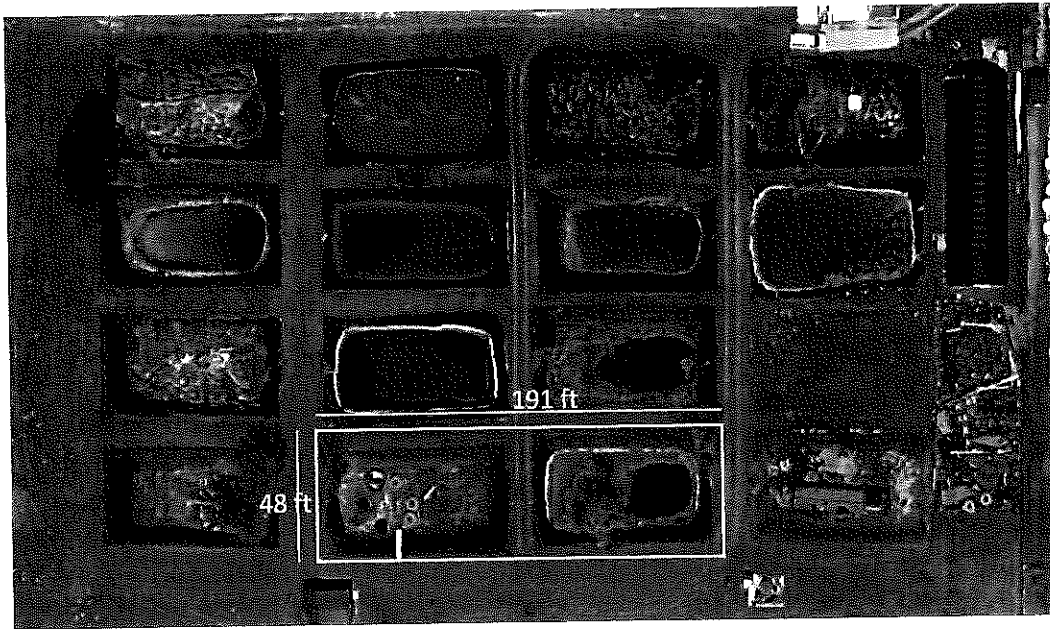


Figure 7. Aerial view of the Aquatic Research Facility study pond location in Norman, Oklahoma.

3.1.1 Experimental Setup

The full-scale controlled mesocosm FWB system was developed based on a modified Y-frame model design. The design consisted of a 10-ft by 5-ft rectangular frame made of 4-inch polyvinyl chloride (PVC) pipe. The ballasts were also made of 4-inch PVC pipes and were attached 2 inches below the main frame. A 6-inch layer of Polyflo filter material (Americo Manufacturing Company Inc., Acworth, GA) was placed inside the rectangular frame. The number of pipes in the skirt wall varied between 0, 6 and 11 pipes. The length of the pipes in the skirt wall varied between 0.0, 1.0, 2.0 and 3.0 ft. Two FWBs adjacent to each other were fastened together on one side and positioned perpendicular to the direction of incoming waves. Figures 8, 9 and 10 below are schematics of the FWBs, and Figure 11 shows an upside-down FWB frame out of the water and being prepared for the next set of frame parameters to be tested.

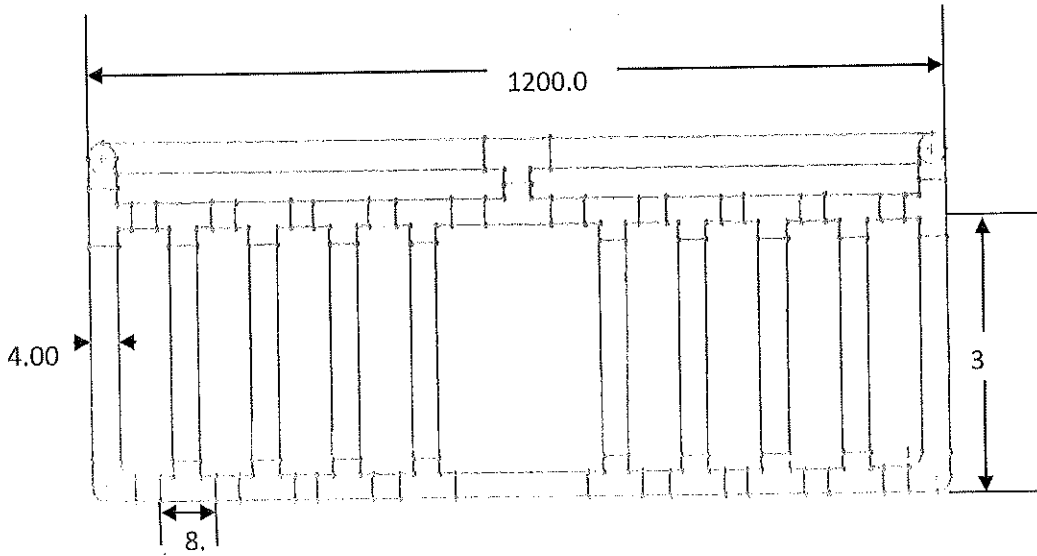


Figure 8. Cross-sectional view of the prototype floating wetland breakwaters showing the dimensions of the pipe ballasts.

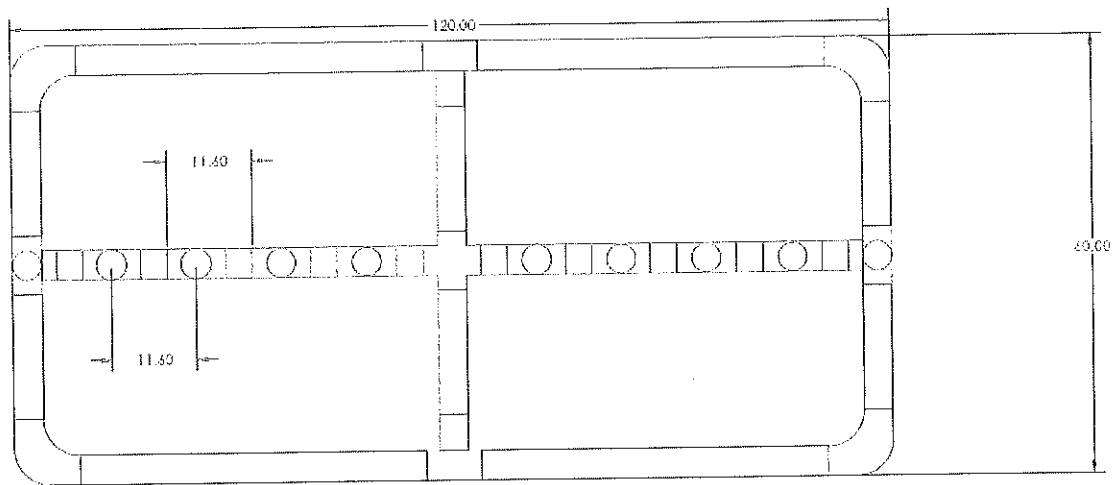


Figure 9. Top view of the prototype floating wetland breakwater frame, showing the top dimensions in inches.

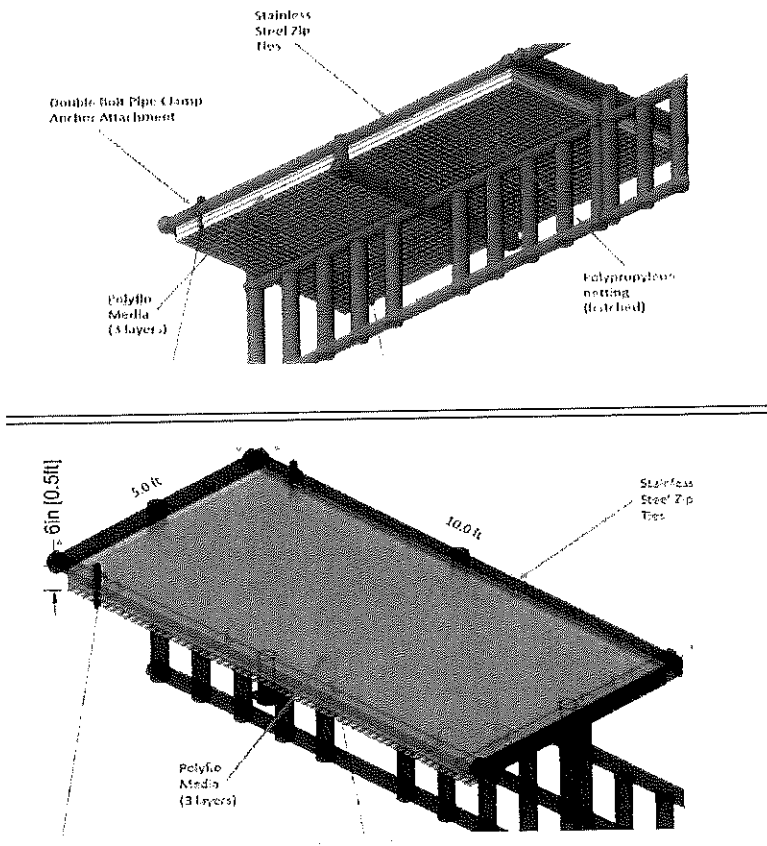


Figure 10. Three-dimensional representation of the FWB design shown from underneath (top) and above (bottom).



Figure 11. Floating wetland breakwater frame used for the prototype system (upside-down). Photo by Maxwell O'Brien.

A wave generator made waves ranging from 3 inches to 14 inches in amplitude. The wave generator, shown in Figure 12, was comprised of paddles attached to a metal frame. The frame was connected by a metal beam to a modified tiller on the back of a John Deere 870 tractor (John Deere, Moline, IL). As the tiller rotated, the beam would push and pull the metal frame, causing the paddles to move back and forth and generate waves in the process. The rotations per minute (RPM) of the modified tiller controlled the frequency of the waves while the stroke length of the modified tiller controlled the wave height. Attaching the metal beam to the outer edge of the tiller would result in a higher radius of rotation and would push the paddles

farther, thus increasing the amount of water moved and the wave height. Each experimental combination of number of pipes and pipe length was subjected to different wave heights during runs. The system was maintained in deep wave conditions, which is defined as the depth of the water is greater than half the wavelength of the water waves (Thurman & Trujillo, 2001). The wavelength was estimated visually, and opportunistically checked from photos and determined to be smaller than double the water depth. The depth of the water in the pond increased from the side of the wave generator to the other end, and was approximately 8 feet at the location where the FWBs were placed in the pond. Waves that travelled through the FWBs had roughly half of the pond length left to travel before reaching the end of the pond. This was done to minimize the reflection of waves (sometimes referred to as bathtub effect), which would affect the wave measurement results. Also, runs were limited to two minutes, which is the approximate minimum time when we would start to see the influence of wave reflection on backside wave measurements. The FWBs were anchored at the four corners using rope and cement blocks, and were sized such that minimal space was present between them and the edges of the pond. Because of the position and anchoring pattern on the FWBs, their only types of motion were pitch (up-down rotation by the transverse or side-to-side axis) and heave (linear up-down motion).

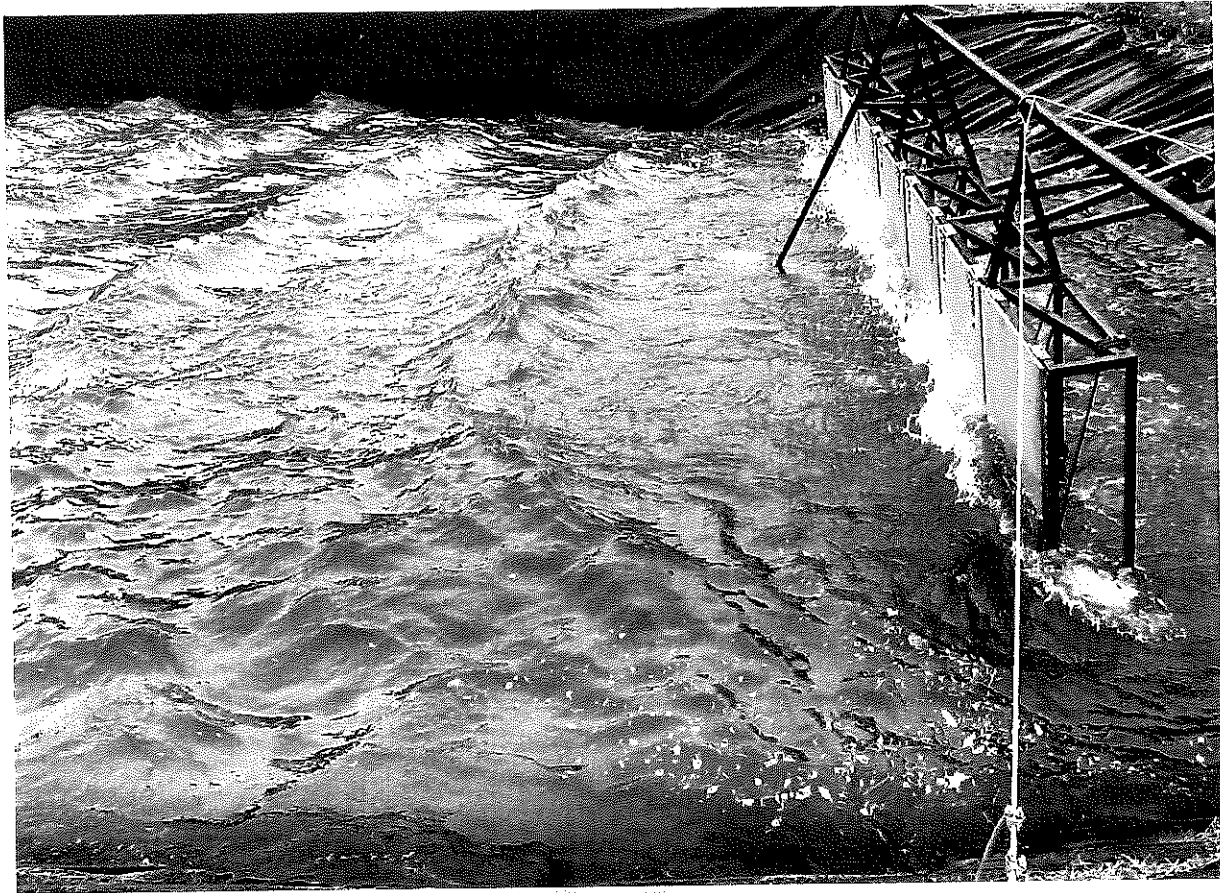


Figure 12. Custom wave generator used for the prototype system. Photo by Maxwell O'Brien.

3.1.2 Wave Height Data Collection

The wave height and period were measured in front of and behind the prototype FWBs during the experimental runs at the ARF. Wave heights were recorded using HERO 7 Black cameras made by GoPro (GoPro, San Mateo, CA), which were attached to meter stick staff gages, which recorded the oscillation of the water level on the meter stick during. The staff gauges were attached to anchors and held vertically at the water surface. Figure 13 shows the experimental setup for the base system. After completion of the run, minimum and maximum heights of each wave were manually recorded and saved in an Excel spreadsheet for analysis.

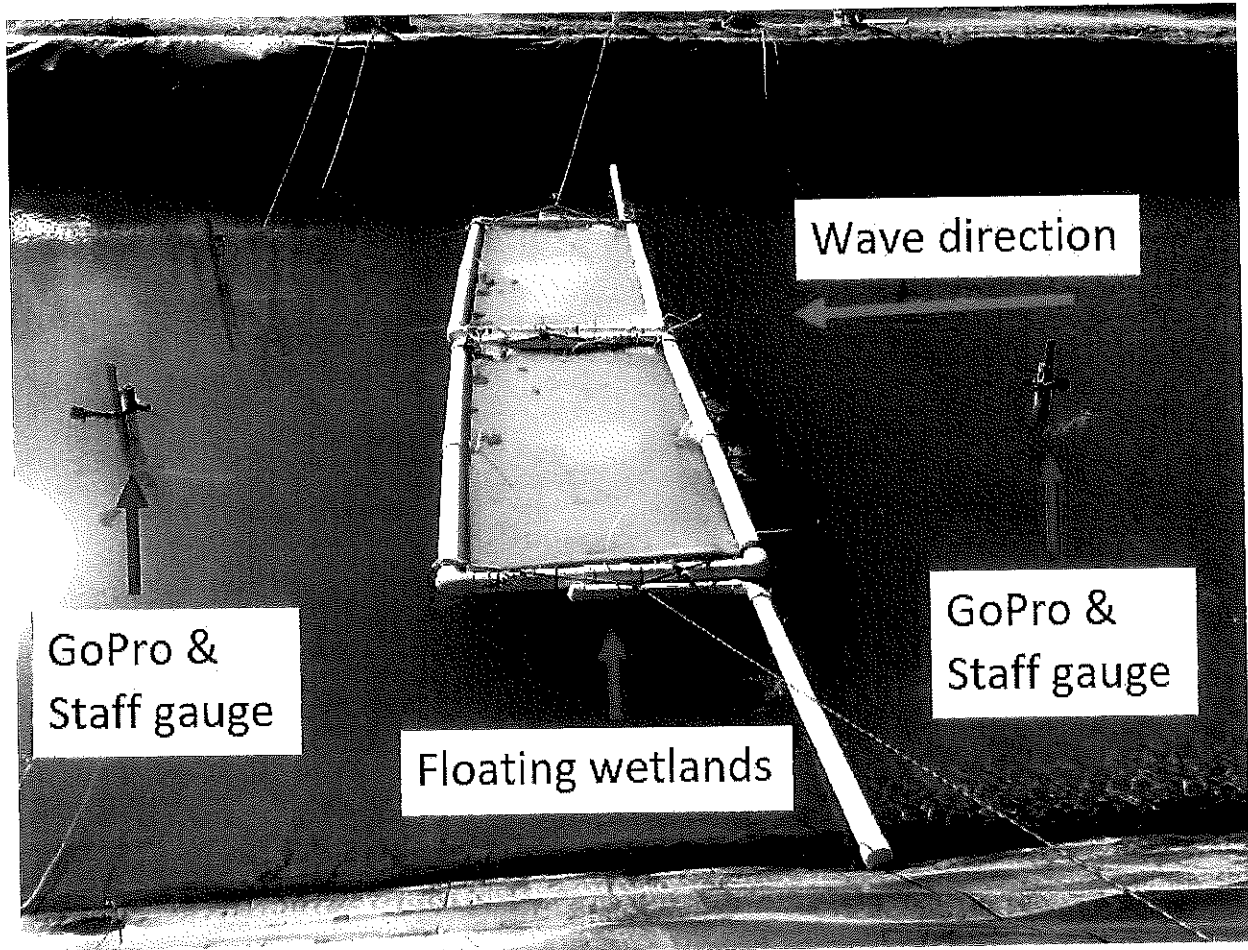


Figure 13. Experimental setup for the full-scale mesocosm system at the Aquatic Research Facility in Norman, Oklahoma. Photo by Maxwell O'Brien.

3.2 Laboratory-scale Controlled Scale Models

Laboratory-scale scale models were tested in laboratory S-22 in Carson Engineering Center at the University of Oklahoma. After properly scaling the FWBs used for the prototype using the Froude number method, the scale model was tested in a flume for waves that were manually generated.

3.2.1 Scaling

The Froude number was used to scale the FWB system from the prototype scale to the small scale. The Froude number is the ratio of inertial forces over gravitational forces and is denoted as,

$$Fr = \frac{u}{\sqrt{gL}}$$

where

- u is the relative flow velocity
- g is the acceleration due to gravity
- L is a representative length of a system such as diameter or width

The Froude number is often used when dealing with free-surface flow systems. It is appropriate here because the FWBs are located at the surface of the water and interact with waves. In order to properly scale a free-surface system like FWBs, an equality of Froude numbers must be achieved between the prototype system and the model. This allows for proper scaling of the FWBs as well as the forces that act on them. A scale of 1:8 based on the length was used for the experiments. All lengths pertaining to the FWB frame, as well as wave heights were scaled by a ratio of 1:8 compared to the initial design to account for geometric similitude. This resulted in FWB frames that were 7.5 in wide. The pipe lengths tested were 0.0, 1.5, 3.0 and 4.5 inches, which correspond to 0.0, 1.0, 2.0, and 3.0 ft pipes, respectively, for the full-scale mesocosm. The length of the frame was not required to be scaled exactly as long as the fraction of the cross section occupied by pipes did not change. It was assumed that the FWB is not required to be longer than the incoming waves, as long as every wave is fully intercepted by the FWB. For example, a wave measuring 6-in across hitting the center of a 12-in long FWB would

be reduced the same as if it hit the center of a 24-in long FWB. The FWB model was constructed to be only slightly smaller than the flume that it was installed in such that the incoming waves would fully be intercepted by the model. On the prototype, the outer diameter of the pipe was 4.5 in and length of the frame was 10 ft, or 120 in. This means that for 11 pipes, the fraction of the length that was obstructed by pipes in the cross section was $(11 * 4.5 \text{ in}) / 120 \text{ in} = 0.41$. For 6 pipes, the fraction was 0.22. At the 1:8 scale, the frames were 23.5 inches long and the pipe outer diameter was 0.84 inches which corresponds to 0.5 in PVC pipe. For the same cross-sectional area obstructed by pipes, the number of pipes were 11 and 6 pipes as shown in Figure 14.

$(0.41 * 23.5 \text{ in}) / 0.84 \text{ in} = 11.47 = 11 \text{ pipes}$ $(0.22 * 23.5 \text{ in}) / 0.84 \text{ in} = 6.15 = 6 \text{ pipes}$

Figure 14. Calculations for the number of pipes for the floating wetland breakwater scale models.

Since the numbers of pipes were rounded, the new fractions of length occupied by pipes and the associated difference were calculated in Figure 15.

$\text{For 11 pipes: } (11 * 0.84 \text{ in}) / 23.5 \text{ in} = 0.39$ $\text{The difference was then: } (0.41 - 0.39) / 0.41 * 100\% = 4.7\%$ $\text{For 6 pipes: } (6 * 0.84 \text{ in}) / 23.5 \text{ in} = 0.21$

Figure 15. Calculations of the errors resulting from the difference in numbers of pipes for the floating wetland breakwater scale models.

For the sake of this experiment, 4.7% was deemed an acceptable level of error. As described by Le Mehaute (1976), the Froude number leads to the following relationship:

$$\left(\frac{V_m}{V_p}\right)^2 = \frac{L_m}{L_p} = \lambda$$

where

V is wave velocity

L is characteristic length

m refers to the scale model

p refers to the prototype or full scale

λ is the scaling ratio which is 1:8 or 0.125

Knowing that wavelength is equal to wave velocity multiplied by wave period, rearranging Equation (2) yields the following relationship:

$$\frac{T_m}{T_p} = \frac{\frac{L_m}{V_m}}{\frac{L_p}{V_p}} = \lambda^{\frac{1}{2}}$$

where T is time frame which corresponds to wave period

By scaling the wave period in the experiments by a factor of $(1/8)^{1/2}$, the velocity and wavelength were properly scaled. The wave periods observed at the prototype scale varied between 1.3 and 2.3 seconds. As a result, the target wave periods used in the 1:8 scale experiments were between 0.46 and 0.81 seconds.

Dynamic similitude between the prototype and the model was not fully achieved because the FWBs at the prototype scale had metal connectors in the skirt wall whereas the model scale FWBs had PVC connectors. This resulted in a density discrepancy in the scaling and could have yielded better wave reduction results for the FWBs at the prototype scale.

3.2.2 Experimental Setup

The model-scale experiments were conducted in a 7.0 ft x 2.0 ft x 2.0 ft flume (Figure 16). Deep-wave conditions, where the water depth is greater than half of the wavelength of the incoming waves, were maintained in all runs. The wavelength was estimated visually and determined to be smaller than double the known water depth. The FWBs were anchored with small bungee cords attached to Marshalltown 4.5-in diameter, 15-lbs blue rubber tile suction cups (Marshalltown, Marshalltown, IA) at the four corners of the frame. Experiments at both scales used this anchoring pattern. Waves were generated on one end of the flume by manually raising and lowering a piece of wood in the water at a constant pace. The waves then traveled towards the other end of the flume. Artificial plants and Polyflo filter material were placed at the end of the flume to dissipate the wave energy and prevent wave reflection.

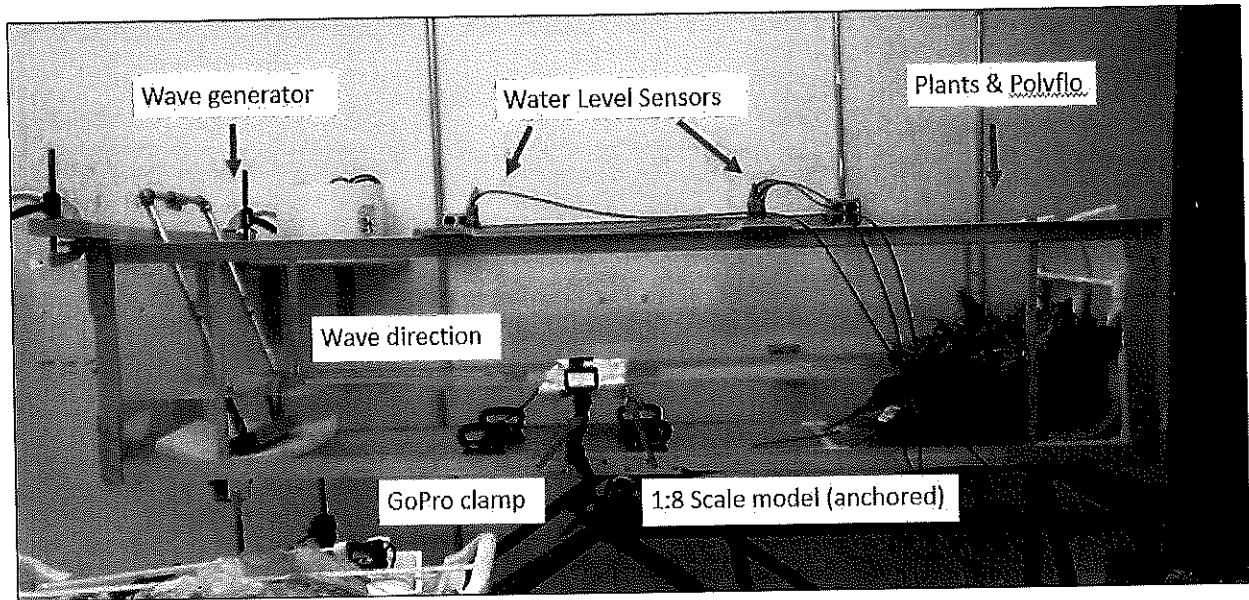


Figure 16. Experimental setup for the scale model similitude studies in Carson Engineering Center at the University of Oklahoma.

3.2.3 Wave Height Data Collection

Wave heights and periods were measured using Senix Toughsonic 3 (Senix Corporation, Hinesburg, VT) ultrasonic water-level sensors. The sensors were placed above the water surface and measured depth to water on a continuous basis. These sensors measured the wave heights in front of and behind the FWB scale model and were synchronized to take simultaneous measurements. To validate the data from the ultrasonic sensors, a HERO 7 Black GoPro captured videos of selected runs. Meter sticks were placed in front of and behind the FWB so that wave peaks and troughs could be estimated on the GoPro videos and recorded in Microsoft Excel (Microsoft Corporation, Redmond, WA). Results from the GoPro videos were then compared with the data from the sensors for validation.

3.3 Field-scale Implementation and Monitoring

The breakwater design chosen from the mesocosm experiments was implemented into Lake Thunderbird during the Spring of 2019 and 2020 at the location seen in Figure 17. One 200 foot long section was installed that was comprised of twenty (20) ten-ft frames and anchored

with twenty, half full, 55-gallon drums of concrete to hold them in-situ. The 200-ft section was chosen because it is approximately the length of the bank that the system is attempting to protect from wind wave and wake action, and for budgetary reasons. In 2019, all frames were outfitted with Polyflo media for plant growth, while in 2020 these systems were modified so that the 5 frames on each end were outfitted with coir matting and the middle ten frames had a modified design for Polyflo media. Proper permissions for the installations were obtained from the US Bureau of Reclamation.

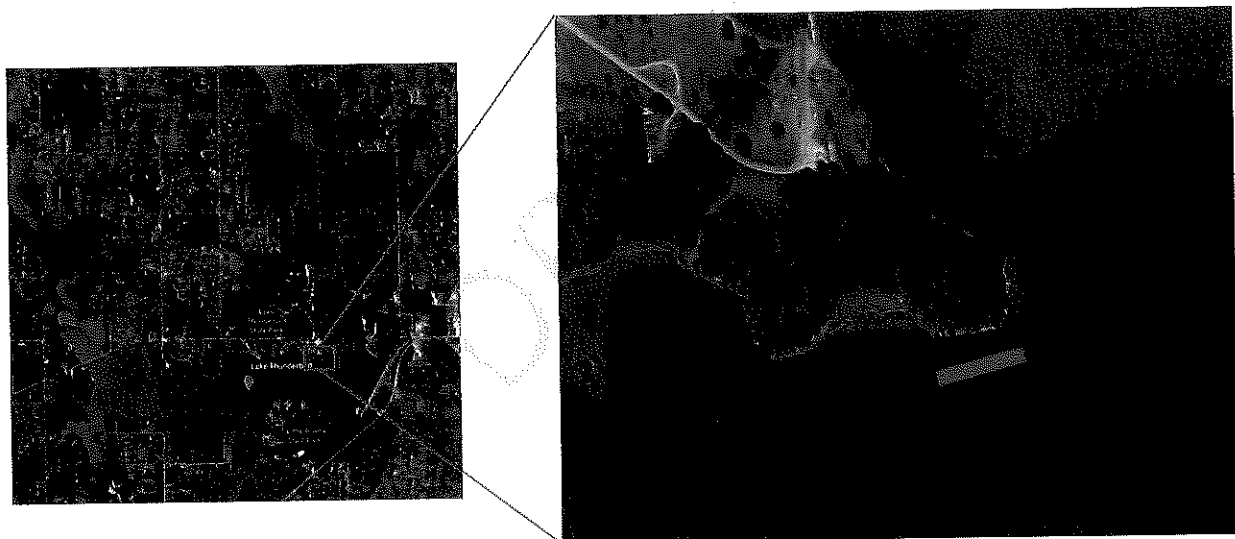


Figure 17. Location of field implementation for the 200-ft floating wetland breakwater. The study location is highlighted by the red rectangle.

Figure 18 shows the overall design of the floating breakwater system illustrating anchor, ADCP, frame, and buoy placement. Note that Figure 18 was the initial plan and shows 22 anchors, however during installation it was decided that 20 anchors would be sufficient because of the available sites for anchor attachment. Each one of the wetland frames were planted

initially with Soft Rush (*Juncus effusus*) and then later supplemented with American water-willow (*Justicia Americana*).

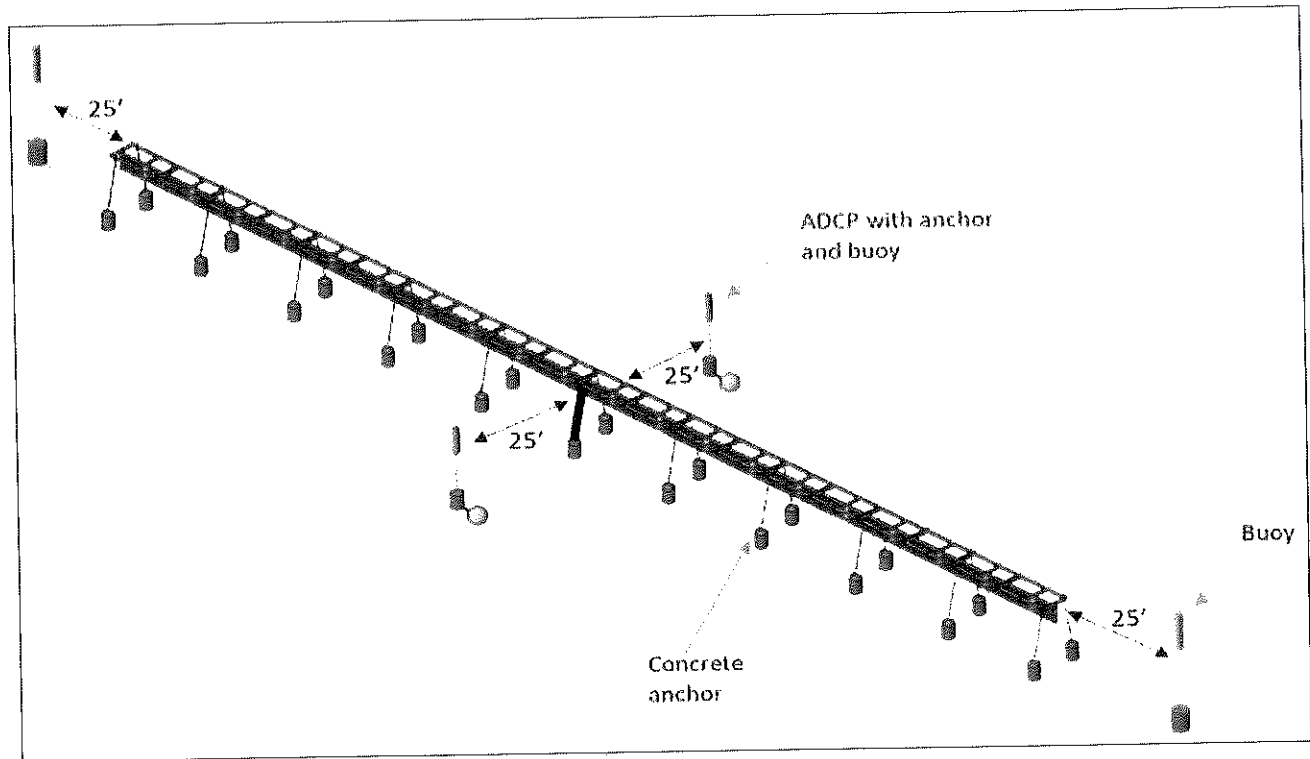


Figure 18. Diagram of the design of the 200-ft section of floating wetland breakwater installed into Lake Thunderbird, including anchors and buoys.

3.3.1 Wave Height Data Collection

Wave height data at the field study location in Lake Thunderbird was collected from a period of August 2020-February 2021. As previously mentioned, ADCPs were initially attempted to be utilized for wave-height data collection. However, due to time constraints and technical issues with the units the decision was made to return to GoPro video analysis. GoPro cameras were attached to a staff gauge inside (near bank) and outside the FWBs to compare the wave height reduction across the FWBs. Data was collected when the predominant wind direction was coming from the Southeast to Southwest, with the goal of capturing waves that are

crossing approximately perpendicular to the floating wetland structure. Furthermore, additional data was collected by creating artificial waves with a boat to simulate wave pulses through the floating wetlands.

In addition to the GoPro analysis, we were able to collect supplementary wave height measurements using photographs from specific days where we already had GoPro video data from the backside of the wetlands using a pixel ruler (<https://www.rapidtables.com/web/tools/pixel-ruler.html>). These wave statistics for this method were validated using historical Mesonet wind data for the area and the following equation:

$$H_f = \frac{\lambda_5 u^2}{g}$$

where

H_f is the height of a fully formed wave

λ_5 is the dimensionless coefficient approximately equal to 0.27

u is the wind speed

g is the acceleration due to gravity

3.3.2 Biological Sampling

Once the FWBs have been positioned and anchored in the locations, opportunistic biological monitoring was opportunistically completed in an attempt to understand the full capabilities of these systems. The FWBs were monitored for their capabilities as a fish habitat by taking fish surveys with the assistance of Steve O'Donnell and the Oklahoma Department of Wildlife Conservation. Additionally, handheld GreenSeeker measurements for normalized difference vegetation index (NDVI) were measured from a constant height of 2.5 ft above selected frames during the fall of 2020 to assess plant survivability in the two different media.

3.3.3 Jet Erosion Test

A Jet Erosion Test (JET) was also completed on the bank at the FWB location to determine the erodibility parameters of the soil using a JET apparatus and other essential pieces (North Carolina State University Department of Biological and Agricultural Engineering, Raleigh, NC). The remaining portions required to perform the JET and the sampling method were completed per methods described by Hanson and Cook (2004).

3.3.4 Estimation of Wave Energy to Cause Erosion

In order to relate the impact of wave height on bank shear stress; we used Linear Wave (aka Airy Wave) theory. This is applied to fluids that are irrotational or non-breaking wave forms. Wave motion exerts shear on near bank sediment and when wave energy exceeds the critical shear stress for initiation of motion of the sediments, the bank material is scoured. For cohesive material the critical shear stress depends on the degree of compaction. Therefore, the rate at which sediments erode depends on the shear stress exerted on the bank and on the critical shear stress at which erosion is initiated.

Waves approaching a bank are affected by the frictional forces along the bottom. As long as the wave does not break, the transported energy per unit time remains constant. Since the waves in Lake Thunderbird are small, Linear Wave theory was used to compute celerity of propagation and related this to particle velocity near the bottom.

In order to apply Linear Wave theory, some basic assumptions were used. These include: the depth of water is uniform; the wave is periodic with a period defined in seconds; only two-dimensional flow (i.e., horizontal in x-axes and vertical in z-axes); and the Coriolis forces are negligible. Linear Wave theory is an approximation of wave propagation by neglecting boundary layer effects that occur near the bed, neglecting viscous and turbulent stresses so that wave

motion is considered fully irrotational; and the wave amplitude is relatively small compared to the wave length.

To determine the celerity of propagation, c , the wave length is related to the period:

$$c = \frac{\lambda}{T}$$

where λ is the wave length, in m and T is the period, in seconds. Since this is the distance the wave travels per the time the wave took to travel the same distance; celerity of propagation is often expressed as:

$$c = \sqrt{\frac{g\lambda}{2\pi} \tanh\left(\frac{2\pi D}{\lambda}\right)}$$

where D is the depth of water. Commonly, k_s is known as the wave dispersion coefficient such that

$$k_s = \frac{2\pi}{\lambda}$$

which can be substituted into the celerity of propagation equation for ease of solver computation.

In the following analysis of wave energy induced shear stress, it was further assumed that the energy losses associated with wave refraction and wave shoaling were negligible. Wave will be attenuated in shallow depths via wave energy dissipation through associated with benthos associated friction. Denny (1995) proposed this simple mechanistic approach to Linear Wave theory while noting that the observed rate of energy dissipation would be accumulative as the first derivative of the wave height relative to axial flow (toward bank). The shear stress, τ_b , can be described as:

$$\tau_b = \frac{1}{2} f_w \rho u_m^2$$

where f_w is the dimensionless friction factor that accounts for wave energy dissipation through sediment friction and u_m is the maximum near bed orbital velocity, in m/s. The friction factor is a function of the Reynold's number and the wave amplitude at the bed or the sediment grain size. While there are standard monographs to relate the friction factor with the Reynold's number; the near bed orbital velocity is required. This presents a circular solution; therefore, the approach used herein evaluated the relationship of the shear stress with maximum near bed orbital velocity as a function of the friction factor.

The maximum near bed orbital velocity, u_m , is determined using the approach described by Denny.

$$u_m = \frac{\pi H_o}{T} \left(\sinh \frac{2\pi}{\lambda} \right)^{-1}$$

where H_o is the wave height in m.

4 Results and Discussion

The wave height and energy reduction results provide a baseline of all three scales of wave reduction performance at each of the three scales for the various FWB frame designs. These results are compared across scales and field results are compared to historical wave heights to determine the percentage of waves that would be reduced. Opportunistically collected biological parameters related to the FWBs in the field are also presented.

4.1 Full-scale Controlled Mesocosm

A full-scale controlled mesocosm study of various frame designs with was completed at the ARF, where number and length of pipe ballasts were tested to determine which combination maximized the reduction of incoming wave heights and energy for field implementation.

4.1.1 Wave Height

Wave height comparisons and resulting trendlines for the full-scale mesocosm at the ARF are shown in Figure 19. The individual run results demonstrated a high degree of variability for incoming waves with a range of 4-11 inch average wave height. In general, all designs showed similar wave reduction trends except for the design with 11 pipe ballasts that were 3 feet long. This design demonstrated more average reduction across the approximate 5.5-8.5 inch wave range for which they were tested than the other designs. Even though data collection times were limited to reduce reflection, it is expected that wave reflection from the back of the mesocosm pond at the ARF may have contributed to the high variability of these individual measurements.

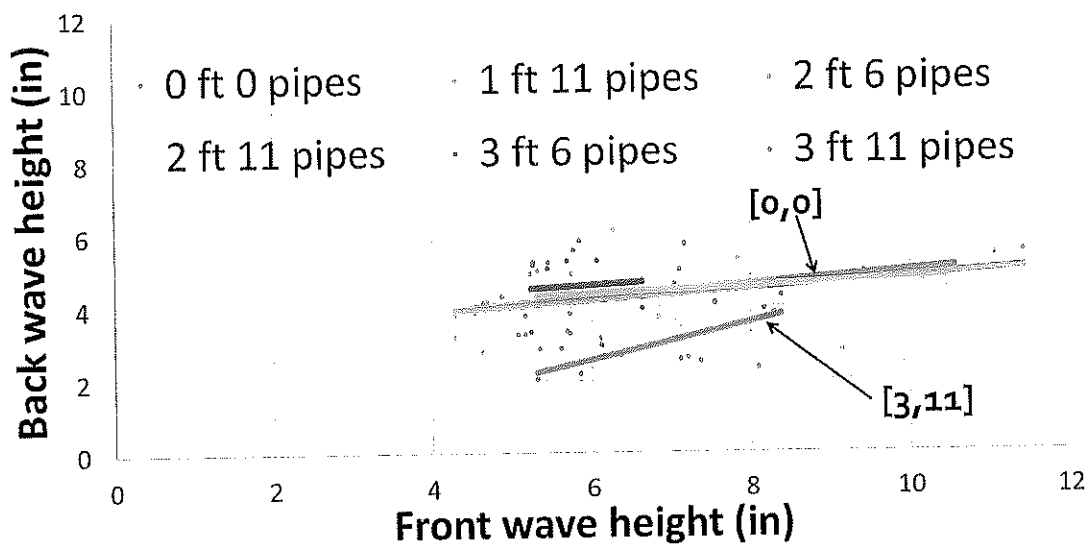


Figure 19. Incoming and outgoing wave height comparisons and linear trendlines for the full-scale mesocosm at the Aquatic Research Facility at the University of Oklahoma in Norman, Oklahoma.

4.1.2 Wave Energy Density

The wave energy density and resulting trendlines for each of the design configurations are shown in Figure 20. Because wave energy density is computed on the critical wave height, which represents the top third of wave heights, the energy trendlines begin to visually separate themselves, with the 3-foot, 11-pipe design still showing the best removal of the designs. Table 2 shows the difference in wave energy density for a six-inch wave based on the trendline predictions for each various designs, showing that the 3-foot, 11-pipe design decreases wave energy by another 45% over having no ballasts/pipes.

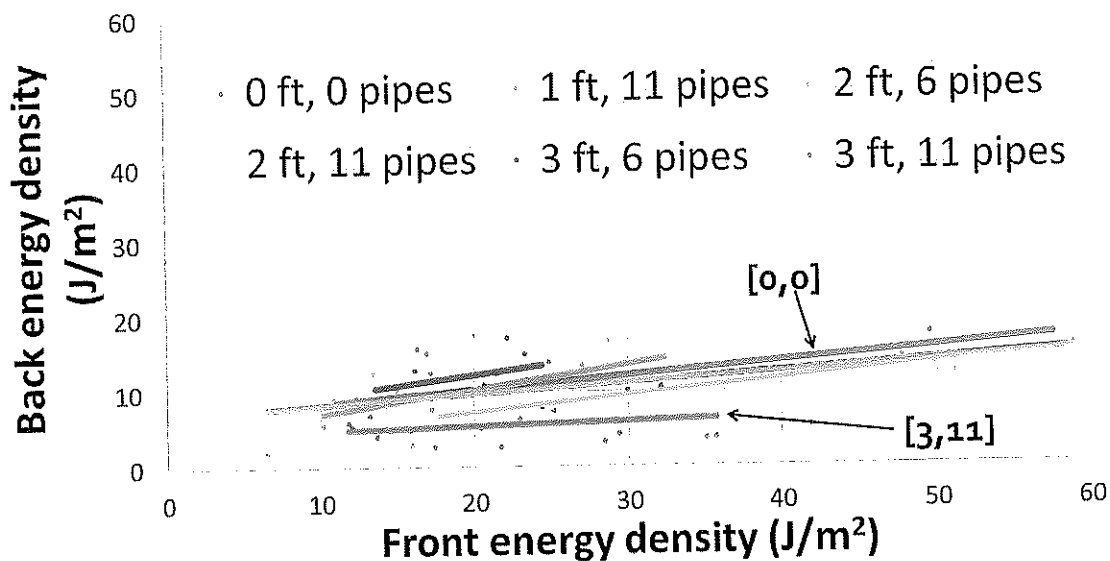


Figure 20. Incoming and outgoing wave energy density comparisons and linear trendlines for the full-scale mesocosm at the Aquatic Research Facility at the University of Oklahoma in Norman, Oklahoma.

Table 2. Wave energy density comparisons for various floating welland breakwater frame designs for a six inch wave. Design configurations show the number and length of pipe ballasts. ** the six pipe, three foot tests represented a limited range of wave height.

Design Configuration	Energy Reduction from [0,0] (J/m ²)
----------------------	---

[0 pipes, 0 feet]	--
[6 pipes, 2 feet]	0.4 (4%)
[6 pipes, 3 feet]	-1.4 (-15%) **
[11 pipes, 1 foot]	0.9 (9%)
[11 pipes, 2 feet]	3.2 (34%)
[11 pipes, 3 feet]	4.3 (45%)

4.1.3 Preliminary Cost Analysis

A preliminary cost analysis (Table 3) was performed comparing the amounts of wave energy reduction to the cost of a ten-foot section of floating wetlands. Materials include pipes, connectors, planting media, and plants. Neither the cost of installation and maintenance nor the time value of money is included in these preliminary calculations. The FWB design with the lowest cost per energy density reduction, which was 11 pipe ballasts that were three foot long, was chosen for implementation in Lake Thunderbird.

Table 3. Preliminary cost analysis based on price per 10-ft length of material and the corresponding amounts of wave energy density reduction, based on a six-inch wave. The bolded selection indicates the design that was selected for field implementation.

Design Configuration	Estimated Material Cost per 10-ft section	10-ft Section Cost per Energy Density Reduction for a 6-inch wave
[0 pipes, 0 feet]	\$2,080	\$424
[6 pipes, 2 feet]	\$3,040	\$573
[6 pipes, 3 feet]	\$3,145	\$898
[11 pipes, 1 foot]	\$3,190	\$550
[11 pipes, 2 feet]	\$3,205	\$396
[11 pipes, 3 feet]	\$3,220	\$354

4.2 Laboratory-scale Controlled Scale Models

Wave reduction experiments by FWB frames at the 1:8 scale was evaluated in the laboratory. Wave-height and energy-density results are compared between FWB design configurations and between scales. These results demonstrate that as long as similitude relationships are maintained and wave reflectance is limited, laboratory-scale models can be utilized to predict performance in the field.

4.2.1. Wave Height and Energy Reduction

Wave heights and energy densities on the front and back of the various FWB designs were investigated for each scale. Figures 21A-21E and 22A-22E compare the wave height and energy results for the prototype scale and the 1:8 scale. In these figures, the results are normalized for scale. This means that for the 1:8 scale, wave-height values were multiplied by 8 and wave-energy density values were multiplied by 64.

Visually, most of the trendlines for the wave height and the wave-energy density graphs overlap. This would suggest that the wave reduction performance of FWBs at different scales is comparable. The outlier is for the 3.0 ft., 11 pipes frame where the trendlines are distinct from each other on the wave height as well as the wave-energy density graphs (Figures 21E and 22E). This frame is the exception in this data set and suggests that the prototype scale performed better than the 1:8 scale as the trendline for the prototype data is placed lower than that of the 1:8 scale data.

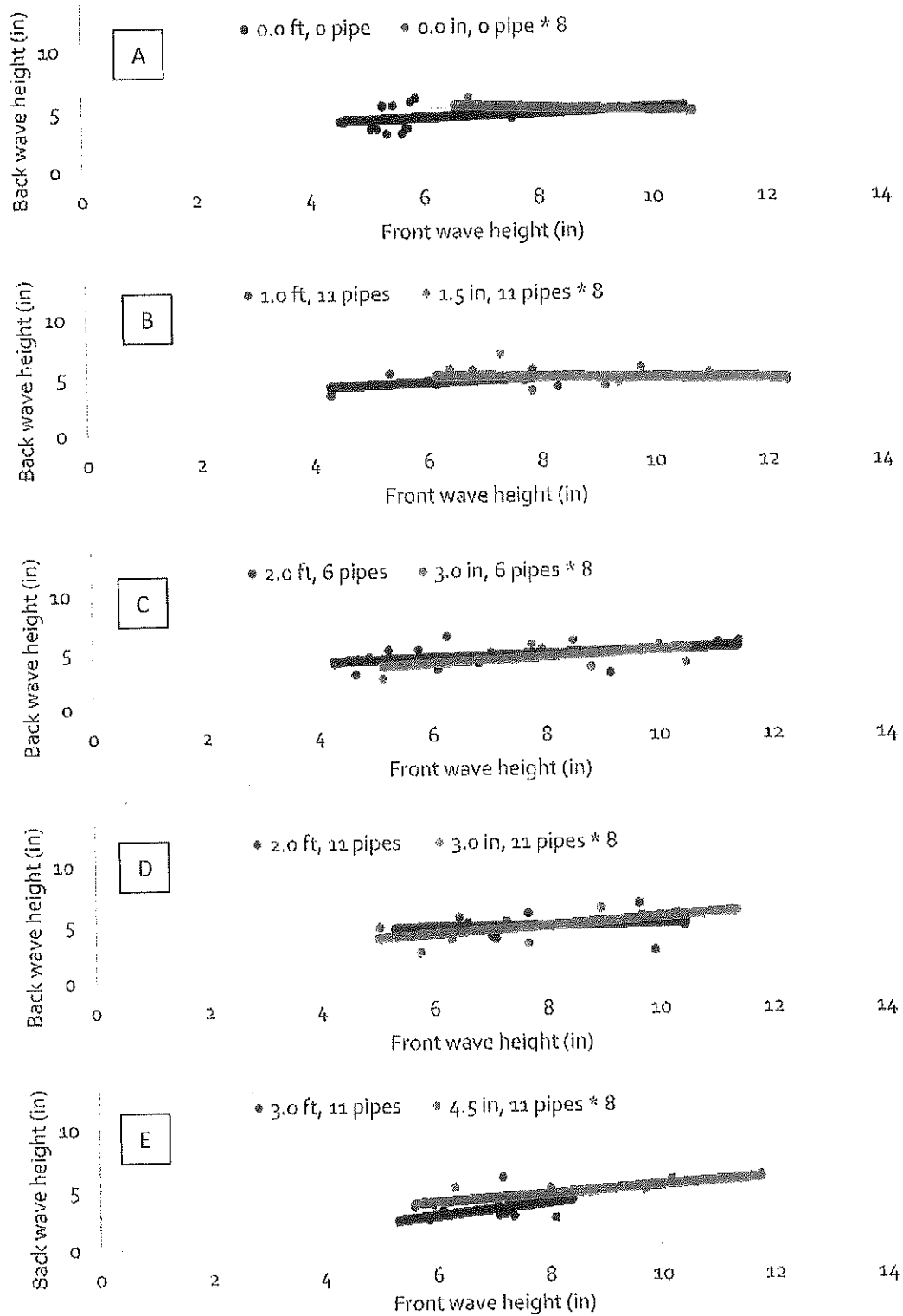


Figure 21. Front and back average wave height comparisons for the full-scale and 1:8 scale for (A) no pipe design, (B) 11 pipes, 1 foot long design, (C) 6 pipes, two foot long, (D) 11 pipes, 2 foot long, and (E) 11 pipes, 3 foot long.

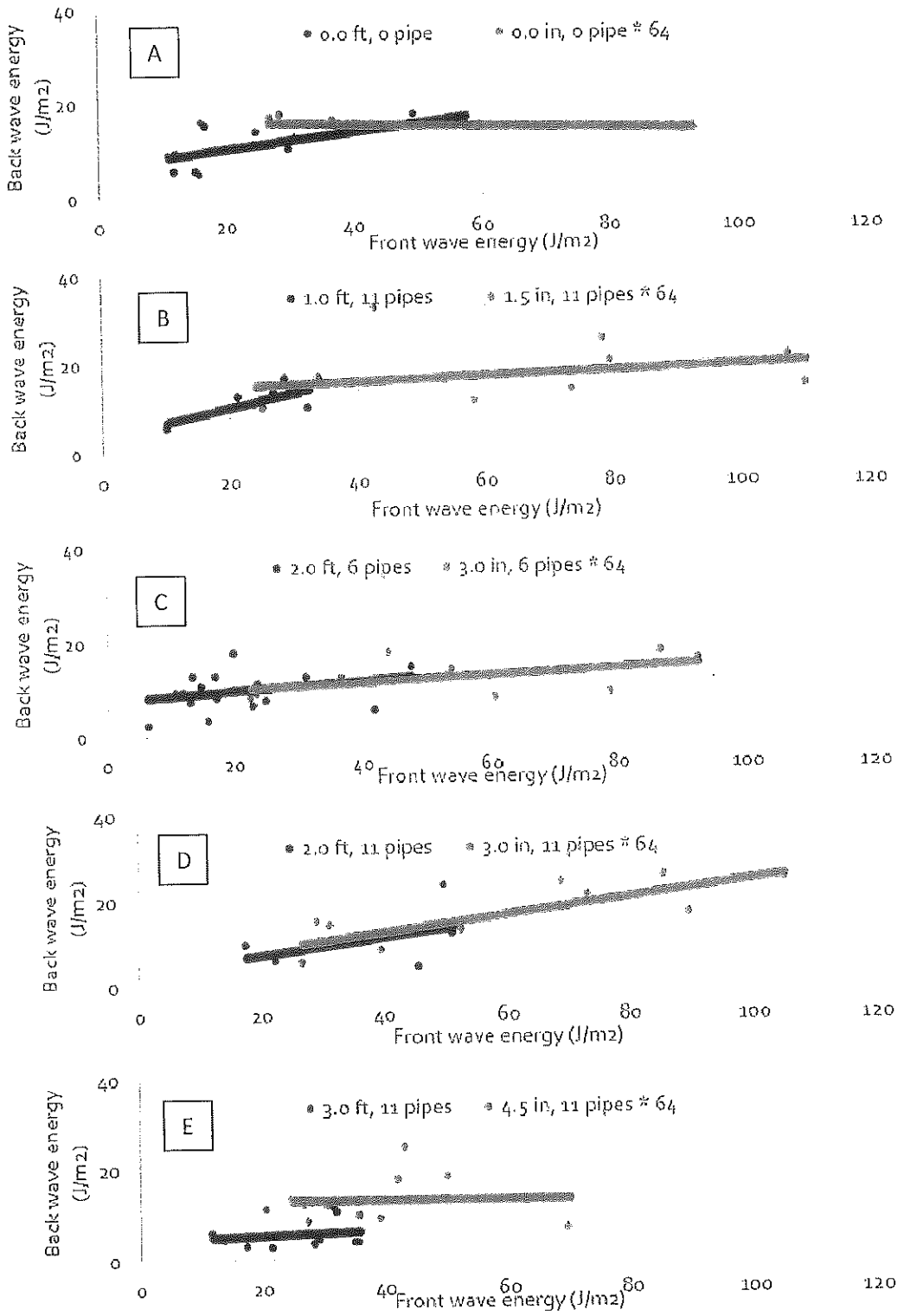


Figure 22. Front and back average wave energy density comparisons for the full-scale and 1:8 scale for (A) no pipe design, (B) 11 pipes, 1 foot long design, (C) 6 pipes, two foot long, (D) 11 pipes, 2 foot long, and (E) 11 pipes, 3 foot long.

The Mann-Whitney U test was used to compare the wave height and wave-energy density between the full-scale mesocosm scale and the 1:8 laboratory scale for the different FWB design configurations (Table 4). The Mann-Whitney U test resulted in no significant difference ($p < 0.05$) in wave height reduction between the prototype scale and the 1:8 scale FWB frames except for the 0.0 ft, 0 pipe frame for wave height, 2.0 ft 6 pipes frame for wave energy density, and the 3.0 ft, 11 pipes frames for both wave height and wave energy density. As mentioned in the visual analysis, the 3.0 ft 11 pipes distribution appears to demonstrate better wave reduction than the other frame configurations at the prototype scale, whereas at the 1:8 model scale it performed similarly to the other frames. The 3.0 ft 11 pipes frame seems to be an exception in these comparisons, and may be a result in differences in scaled weight per length at the two scales, as the relative width and density of PVC at these two scales is different, especially when for large number of pipes and connections in each system. If the experiment were repeated, we would record their linear weights (mass/length) to ensure that they compared relative to force similitude.

Table 4. p values for Mann-Whitney U test comparing prototype scale and 1:8 model scale wave height and wave-energy density distributions for different floating wetland breakwater frame ballast configurations.

	Pipe Ballast configuration	p-value
Wave height	0.0 ft 0 pipe	0.01
	1.0 ft 11 pipes	0.64
	2.0 ft 6 pipes	0.51
	2.0 ft 11 pipes	0.65
	3.0 ft 11 pipes	<0.01
Wave-energy Density	0.0 ft 0 pipe	0.09
	1.0 ft 11 pipes	0.06
	2.0 ft 6 pipes	0.04
	2.0 ft 11 pipes	0.18
	3.0 ft 11 pipes	<0.01

To investigate the effect of pipe length and number of pipes on FWB wave reduction, the Mann-Whitney U test was used to compare the wave height and energy density results from the different FWB configurations tested to one another. Tables 5-8 show the p-values for the Mann-Whitney U test comparing these FWB configurations. The results indicate that there is generally no significant difference in wave height and energy density reduction between the different FWB configurations tested, except for the 3.0 ft 11 pipes configuration in the field, which is significantly different from those of all other configurations at the prototype scale for both wave height and wave energy density. At the model scale, the 1.5 in 11 pipes configuration and the 3.0 in 6 pipes configuration are also significantly different when comparing wave energy density results. The 3.0 in 6 pipes configuration seems to perform better than the 1.5 in 11 pipes configuration, although this may be an artifact of the data related to a relatively small sample set.

Table 5. p values from Mann-Whitney U test comparing wave height reduction of different floating wetland breakwater (FWB) configurations at the laboratory 1:8 model scale. p values less than 0.05 are highlighted and are considered significantly different.

FWB configuration	0.0 in, 0 pipe	1.5 in, 6 pipes	1.5 in, 11 pipes	3.0 in, 6 pipes	3.0 in, 11 pipes	4.5 in, 11 pipes
0.0 in 0 pipe		0.13	0.25	0.17	0.23	0.10
1.5 in 6 pipes			0.69	0.80	0.87	0.77
1.5 in 11 pipes				0.31	0.98	0.39
3.0 in 6 pipes					0.63	0.85
3.0 in 11 pipes						0.65

Table 6. p values from Mann-Whitney U test comparing wave energy density reduction of different floating wetland breakwater (FWB) configurations at the laboratory 1:8 model scale. p values less than 0.05 are highlighted and are considered significantly different.

FWB configuration	0.0 in, 0 pipe	1.5 in, 6 pipes	1.5 in, 11 pipes	3.0 in, 6 pipes	3.0 in, 11 pipes	4.5 in, 11 pipes
0.0 in 0 pipe		0.25	0.85	0.17	0.88	0.61
1.5 in 6 pipes			0.78	0.05	0.67	0.18
1.5 in 11 pipes				0.04	0.54	0.22
3.0 in 6 pipes					0.25	0.31
3.0 in 11 pipes						0.61

Table 7. *p* values from Mann-Whitney U test comparing wave height reduction of different floating welland breakwater (FWB) configurations for the full-scale mesocosm. *p* values less than 0.05 are highlighted and are considered significantly different.

FWB configuration	0.0 in, 0 pipe	1.5 in, 6 pipes	1.5 in, 11 pipes	3.0 in, 6 pipes	3.0 in, 11 pipes
0.0 ft 0 pipe		0.80	0.95	0.37	0.001
1.0 ft 11 pipes			0.72	0.55	0.012
2.0 ft 6 pipes				0.44	0.001
2.0 ft 11 pipes					0.005

Table 8. *p* values from Mann-Whitney U test comparing wave energy density reduction of different FWB skirt wall configurations for the full-scale mesocosm.. *p* values less than 0.05 are highlighted and are considered significantly different.

FWB configuration	0.0 in, 0 pipe	1.5 in, 6 pipes	1.5 in, 11 pipes	3.0 in, 6 pipes	3.0 in, 11 pipes
0.0 ft 0 pipe		0.83	0.79	0.88	0.006
1.0 ft 11 pipes			0.58	0.66	0.01
2.0 ft 6 pipes				0.93	0.006
2.0 ft 11 pipes					0.02

4.3 Field-scale Implementation

The mesocosm scale tests resulted in a design that produced the most cost-efficient wave height and energy reduction amongst our tested designs. That design was implemented in a 200-ft-long section into Lake Thunderbird in the Spring of 2019. These FWBs were monitored for wave height and energy reduction, along with opportunistic measurements of other biological parameters including fish and wildlife habitat and a measure of live green vegetation coverage.

4.3.1 Wave Height and Energy Reduction

Critical wave height and energy reductions were evaluated through a combination of ADCP data, GoPro video, and image analysis. Figure 23 shows the average front-wave heights

compared to the corresponding wave heights after the waves had passed through the FWBs for eight different measurement periods.

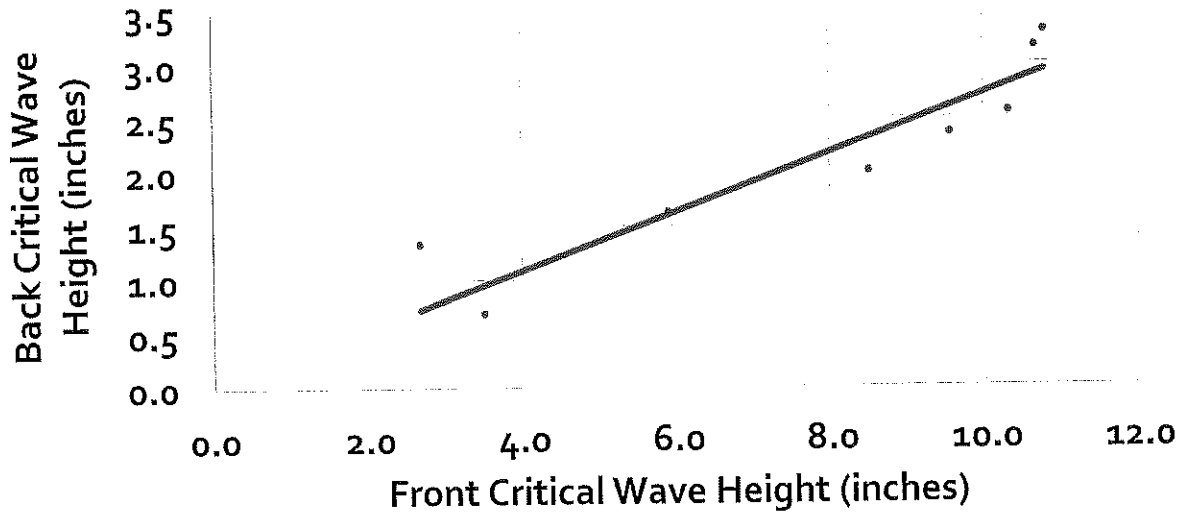


Figure 23. Comparison of the average critical wave height before and after a wave crosses the floating wetland breakwaters installed at Lake Thunderbird.

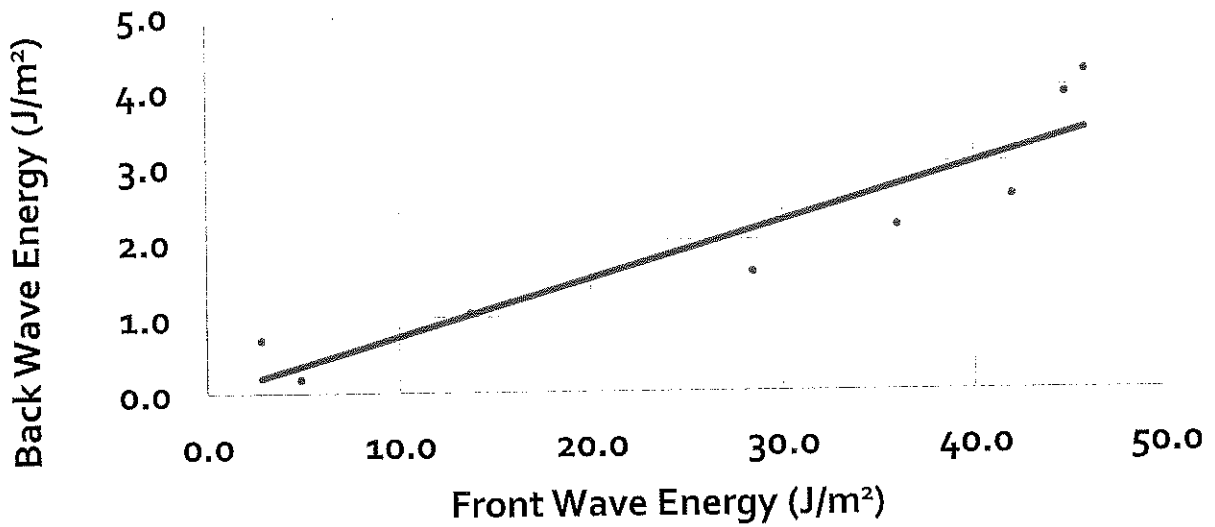


Figure 24. Comparison of the average wave energy density before and after a wave crosses the floating wetland breakwaters installed in Lake Thunderbird.

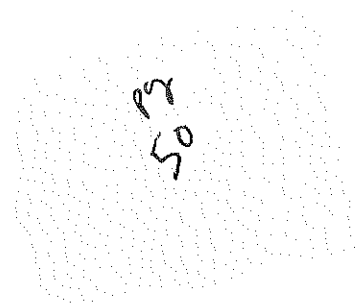
In addition to wave-height reduction, an energy-density reduction analysis was also performed on the collected wave-height data, as shown in Figure 24. On average, FWBs caused 70-80% reduction in wave height and 91-94% percent reduction for wave energy density. These field-scale results demonstrated greater wave reduction than the full-scale controlled study at the ARF. These results will be further discussed later in this report comparing all three scales of this study.

4.3.2 Estimation of Long-term Erosion Minimization at the Study Bank

The long-term minimization of forces that can cause detachment erosion was completed by combining JET test results with wave height estimations based on 5-minute weather data from the Norman, Oklahoma Mesonet site.

4.3.2.1 Jet Erosion Test (JET) Results

A JET was performed on the bank where the FWBs were located. Following the procedure outlined in Hanson and Cook (2004) and the JET Spreadsheet tool provided by Dr. Garey Fox from the North Carolina Department of Biological and Agricultural Engineering. Results of this analysis are shown in Figure 25.



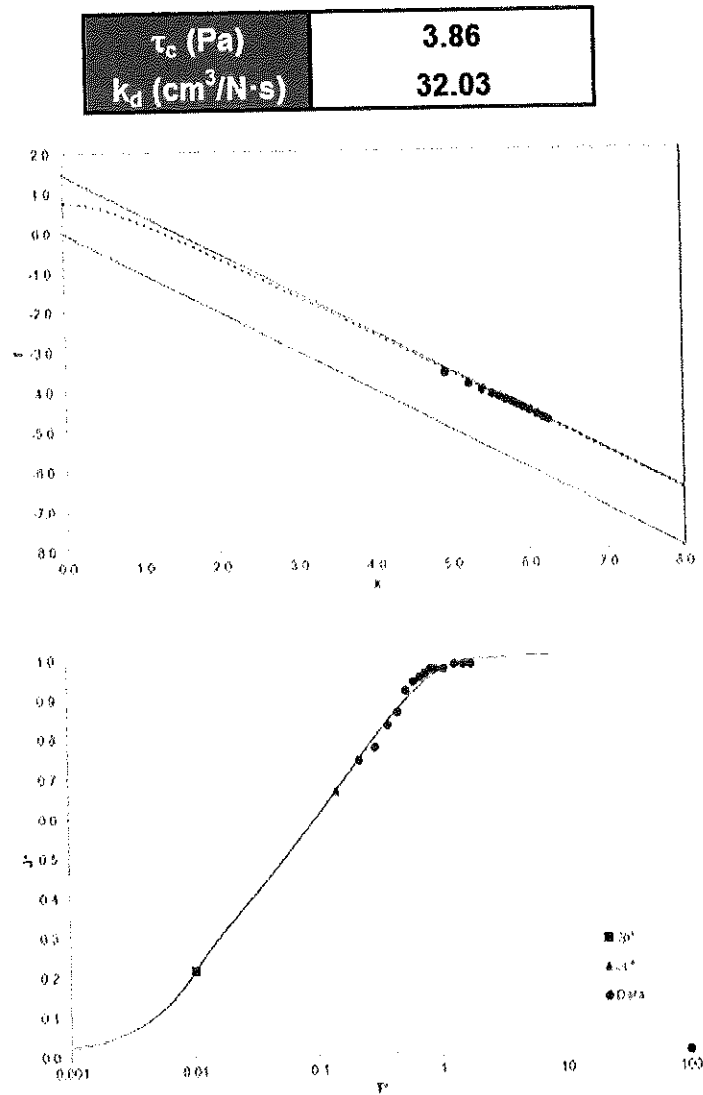


Figure 25. Jet erosion test (JET) comparison graph showing the observed values collected in the field to the three JET solutions.

Upon visually inspection of the results produced from the spreadsheet tool the Scour Depth Solution was used to estimate erosion parameters. Based on this solution, the erodibility coefficient (K_d) was estimated to be $32.0 \frac{\text{cm}^3}{\text{N}\cdot\text{s}}$ and the critical shear stress t_c was estimated to be 3.86 Pa. The wave height that would begin detachment erosion at our study bank was estimated using linear wave theory as described earlier. These calculations resulted in a 3.1-inch wave to

be required for the beginning of soil detachment at the study bank. It is important to note that this does not necessarily mean that significant erosion would occur at this wave height, but this wave height could begin to mobilize some sediment. It does also not account for erosion that may occur from mass wasting of wet soils, especially during periods when the reservoir level is dropping.

4.3.2.2 Comparison to Long-term Estimated Wave Heights

To fully understand and estimate long-term erosion process at the study bank, historical wind speed data from 06/2002-03/2021 for the Norman Oklahoma, Mesonet Weather Station were used to estimate predicted fully formed incoming wave heights on our study bank based on wind speed. During this period, the average wind speed out of the Southeast to Southwest directions was 8.9-mph with a standard deviation of 4.94. Figure 26 is the resulting histogram from that data period.

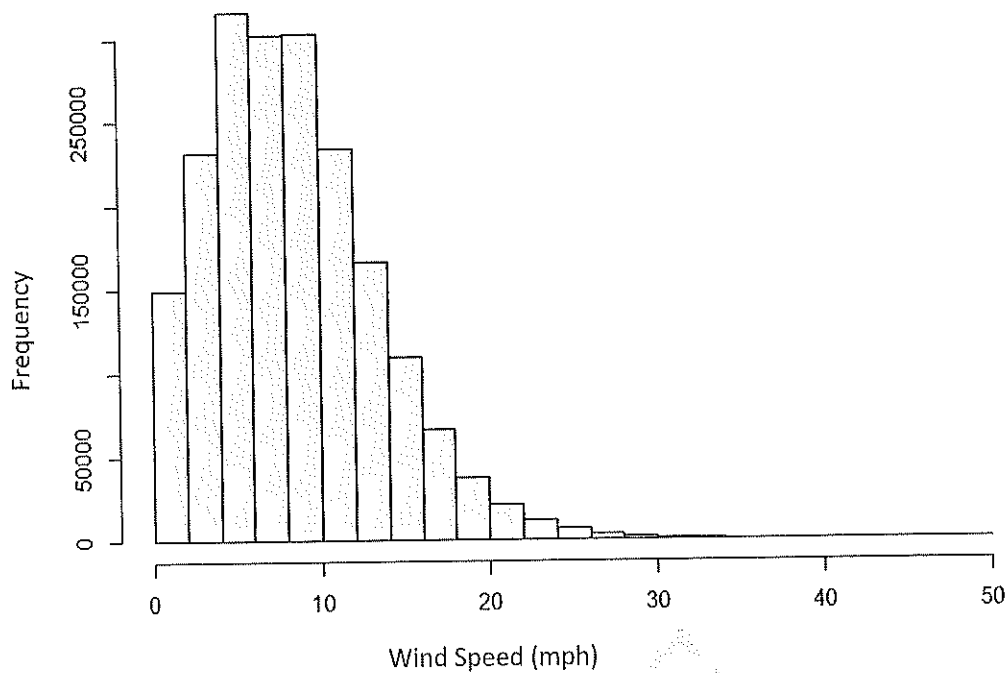


Figure 26. Histogram showing the historical wind speed and the frequency each one occurred for winds from the Southeast to Southwest. (Source: Norman, Oklahoma Mesonet Site)

The 5-minute wind speed data over the past 19 years from the Norman, Oklahoma Mesonet site (https://www.mesonet.org/index.php/sites/site_description/nrmn) were used to predict the fully formed wave height those winds speed would produce at the study location by using the empirical relationship described in section 2.3.1. Table 9 demonstrates the percentage of waves in the range less than 3.1 inches with and without a FWB, using the trendline equation of the data shown in Figure 23 (outgoing wave height = $0.2717 \times [\text{incoming wave height}]$). Adding our floating wetland water system will reduce 96% of the waves hitting that shore to a height that is less than what is required.

Table 9. Percentage of waves in various height ranges with and without floating wetland breakwaters, based on wave height estimations for 5-minute wind speeds from the Norman, Oklahoma Mesonet site (https://www.mesonet.org/index.php/sites/site_description/nrmn)

	No Wavebreak	With Floating Wetland Breakwater, 11 Pipes, 3-ft Length [Field]
Incoming 5-minute Average Wave Height to Give resulting outgoing wave (in), estimated from regression	Percentile	Outgoing Wave Height (in)
3.1	66%	0.8
11.4	96%	3.1
13.0	97%	3.5
47	100%	13

Additionally, the wave reduction potential of these FWB systems, the maximum southerly wind speed recorded between June 2002 and March 2021 was 79 miles per hour (mph) on July 30, 2003, which would result in a wave height of approximately 1.2 meters or 47 inches. Based on the trendline equation, if the FWBs were in position, they could have potentially reduced that wave height to approximately 13 inches. While this is outside the tested range of our system, if the relationship still holds it does give an approximation of the reduction potential of these systems in high winds. In addition, the top 3% of all waves that hit the bank are reduced to an average height of less than 13 inches in height when our system is implemented.

4.4 Discussion Comparing All Three Scales

4.4.1 Wave Transmission Coefficient Comparison

The wave-height reduction results from this study were compared to those of other studies on floating breakwaters. Wave height reduction is often calculated using the wave

transmission coefficient, K_t . The wave transmission coefficient is calculated by the transmitted wave height or back height divided by the incident or front height. The ranges of wave transmission coefficients found in the studies of Neelamani (2018), Uzaki (2011) and Ozeren (2011) were compared to those found in this study at the prototype scale and at the 1:8 scale as shown in Table 10.

Table 10. Range of wave transmission coefficient values (K_t) for floating breakwaters on other studies and the floating wetland breakwater designs investigated in this study.

Source	K _t range			Description
	Prototype scale	Model scale	Field Scale	
Neelamani (2018)	0.6 - 0.8	NA	NA	Pontoon floating breakwater with varying skirt wall sizes
Uzaki (2011)	NA	0.3 - 1.0	NA	Steel pontoon floating breakwater with trusses
Ozeren (2011)	0.2 - 0.9	NA	NA	Cylindrical floating breakwater
Webb (2014)	NA	0.4-1.0	NA	Biohaven floating wetland breakwater without plants
FWB [0.0 ft, 0 pipes]	0.5-1.0	0.7-0.9	NA	Floating Wetland Breakwater with no ballast
FWB [1.0 ft, 11 pipes]	0.5-0.9	0.3-0.9	NA	Floating Wetland Breakwater with pipe ballasts
FWB [2.0 ft, 6 pipes]	0.3-1.0	0.3-0.7	NA	Floating Wetland Breakwater with pipe ballasts
FWB [2.0 ft, 11 pipes]	0.4-0.8	0.4-0.9	NA	Floating Wetland Breakwater with pipe ballasts
FWB [3.0 ft, 11 pipes]	0.3-0.8	0.5-0.8	0.2-0.5	Floating Wetland Breakwater with pipe ballasts

The ranges of wave transmission coefficients found in this study are similar to those found in other studies. The maximum wave transmission coefficients are also similar across studies, except for the study by Neelamani. This suggests that the FWBs used in this study exhibit similar or better performance compared to non-wetland floating breakwaters from these studies. In addition, the field implementation of our chosen frame design with 11 pipes that are

three foot long exhibited the best, consistently low wave transmission values of any reported study.

4.4.2 Comparisons of the Implemented Design at Three Scales

The wave height and energy density reduction from the implemented design to 11 pipe ballasts that were each three foot long for each 10-ft section is shown in Figures 27 and 28, respectively. These results suggest that, even when attempting to account for all similitude-related variables, model simulations are probably a conservative estimate of wave height and energy density reduction. However, these results appear to be predictable, so if one knows the relationship of the results at the various scales then utilizing scale models can still be useful for predicting performance when implemented in the field. Further testing in additional locations would be required to verify this conclusion.

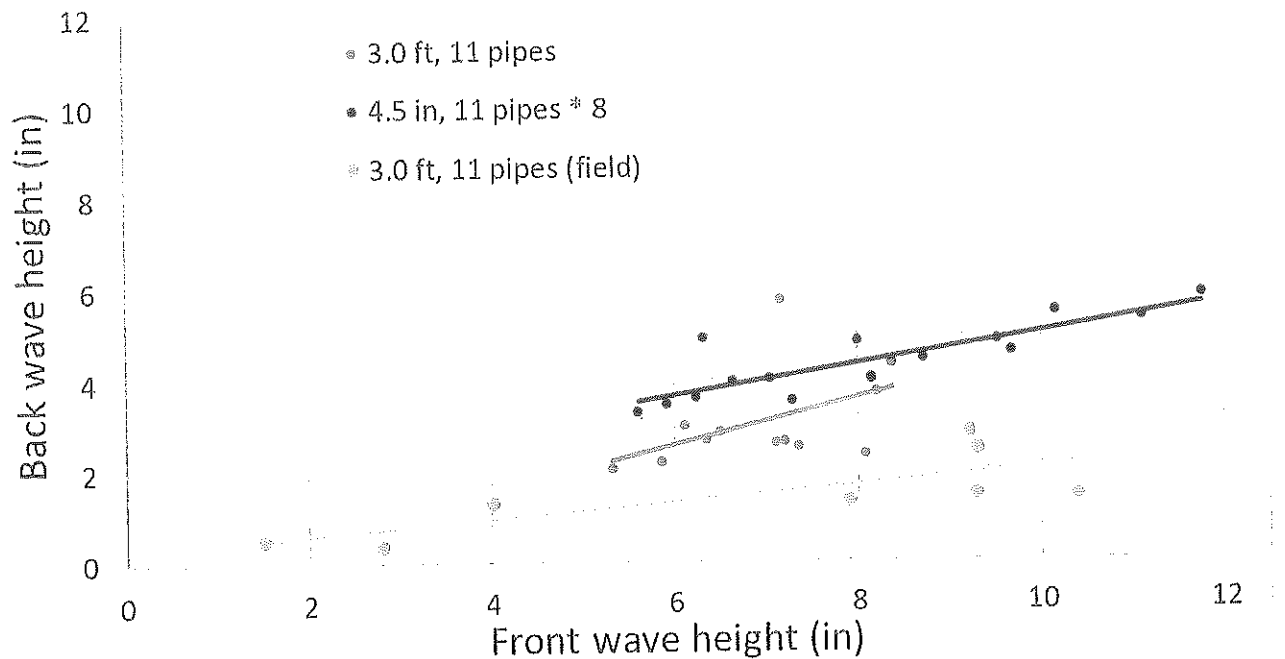


Figure 27. Comparison of wave reduction caused by floating welland breakwaters for all three scales of this study for the implemented design [full-scale mesocosm (blue), laboratory scale (red), and field (yellow)], which had 11 ballast pipes that were 3 feet long.

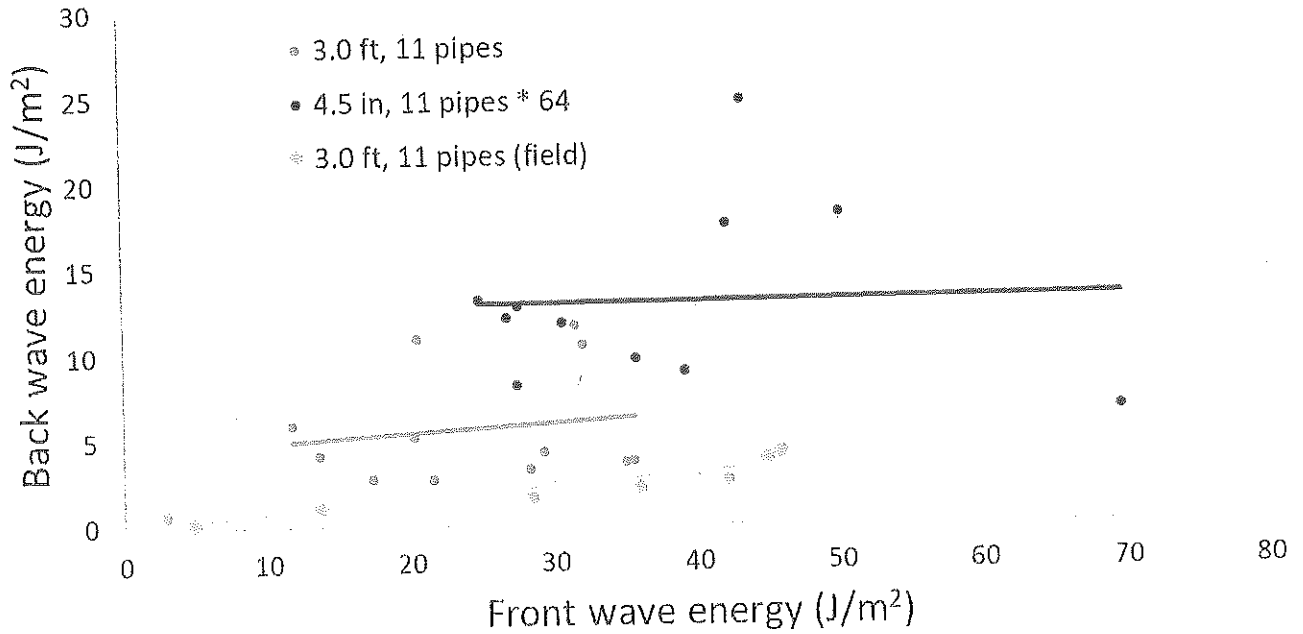


Figure 28. Comparison of wave energy density reduction caused by floating wetland breakwaters for all three scales of this study for the implemented design [full-scale mesocosm (blue), laboratory scale (red), and field (yellow)], which had 11 ballast pipes that were 3 feet long on each 10-foot section.

4.5 Opportunistic Biological Monitoring

4.5.1 Fish Surveys

Two fish surveys were completed around both at the location of the FWBs and the control site further to the West. With assistance from Steve O'Donnell with the Oklahoma Department of Wildlife Conservation, two electrofishing sampling trips were completed at the FWB and a control site to compare the different populations of fish inhabiting each area. Table 11 shows the results of the first sampling trip completed in November of 2019. The control site for these samples was from a location directly to the east of the floating wetland installation in Lake Thunderbird, approximately the same distance from the shore; it is open water, 2-3 meter in depth, with little to no submerged structures. A notable difference between the two locations is the population of Largemouth Bass (*Micropterus salmoides*) at the FWBs compared to the

control site. Considering that Largemouth Bass are commonly concentrated in areas with submerged structures including vegetation, sunken trees, and rocks, the FWBs provide a quality habitat for this ever-popular sport fish (Claussen, 2015). Additionally, species such as the White Crappie (*Pomoxis annularis*) and Blue Gill (*Lepomis macrochirus*) that tend to congregate around submerged structures were also found in more abundance around the FWBs. The control site used in this study is essentially open water, 2-3 meter in depth, with little to no submerged structures which is represented by the fish collected there. Most notably is the higher presence of Gizzard Shad (*Dorosoma cepedianum*) and Silverside (*Menidia beryllina*), schooling bait fish that prefer open water (Miller, 1960). Furthermore, open water predatory fish, such as the White Bass (*Morone chrysops*) and Saugeye (*Sander canadensis x vitreus*) were collected at the control site but did not appear around the FWBs.

The second fish survey (Table 12) was completed in August 2020 and showed similar results to the initial fish survey. Largemouth and other fish that congregate around submerged structures being present at the FWBs and more fish that tend to open water on the control site. It is important to note that the second survey was done in the late summer where the water temperatures were still relatively warm, meaning that some fish may have still been in the deeper, cooler water and not moved to the shallower water around the frames at this time. During the 2020 fish survey a school of gizzard shad swam across the path of the boat, so after the first 40 Gizzard Shad collected it was decided that no more were required to get a comprehensive example of the type of fish present at each location. FWBs show promise as a suitable habitat for many different types of fish species. They offer a recreational aspect to the system as fishermen may be drawn to the area in search of that prized sportfish. With FWBs continuing to show promise as wave breaks, and with the added benefit of fish and wildlife

habitat to an area with severely eroded banks adds to the restoration potential of these systems. It is also expected that after the plants are established they will attract an even wider diversity of fish, as has been seen in other studies.

Table 11. Fish survey results from the floating wetland breakwater and control site, completed in November 2019.

Lake Thunderbird Fish Survey Results (2019)					
Floating Wetland Breakwaters (FWBs)			Control		
Species	Count	Mean Length (mm)	Species	Count	Mean Length (mm)
Bluegill	2	158	Bluegill	0	0
Channel Catfish	1	372	Channel Catfish	0	0
Common Carp	1	508	Common Carp	1	660
Flathead Catfish	0	0	Flathead Catfish	1	710
Gizzard Shad	2	223	Gizzard Shad	6	216
Largemouth Bass	9	351	Largemouth Bass	2	450
Silverside	2	76	Silverside	7	51
Saugeye	0	0	Saugeye	2	272
White Bass	0	0	White Bass	6	216
White Crappie	1	234	White Crappie	0	0
Total	21		Total	18	

Table 12. Fish survey results from the floating wetland breakwater and control site, completed in August 2020.

Lake Thunderbird Fish Survey Results (2020)					
Floating Wetland Breakwaters (FWBs)			Control		
Species	Count	Mean Length (mm)	Species	Count	Mean Length (mm)
Bluegill	1	147	Bluegill	0	0
Channel Catfish	1	290	Channel Catfish	0	0
Gizzard Shad	15	185	Gizzard Shad	40	184
Largemouth Bass	2	329	Largemouth Bass	0	0
White Bass	2	250	White	1	250
Total	25		Total	41	

4.5.2 Plant Monitoring

In limited opportunistic monitoring, plants in PolyFlo maintained their greenness better than plants in the coir mattresses during a two-month period in September and October 2020 (Figure 29), as measured using NDVI values measured using a GreenSeeker at a constant height of 2.5 feet above the frames over time. These data confirm the visually weekly or sometime daily inspection of the FWBs, where the PolyFlo appeared to hold and protect the wetland plant species better than the coir during this period.

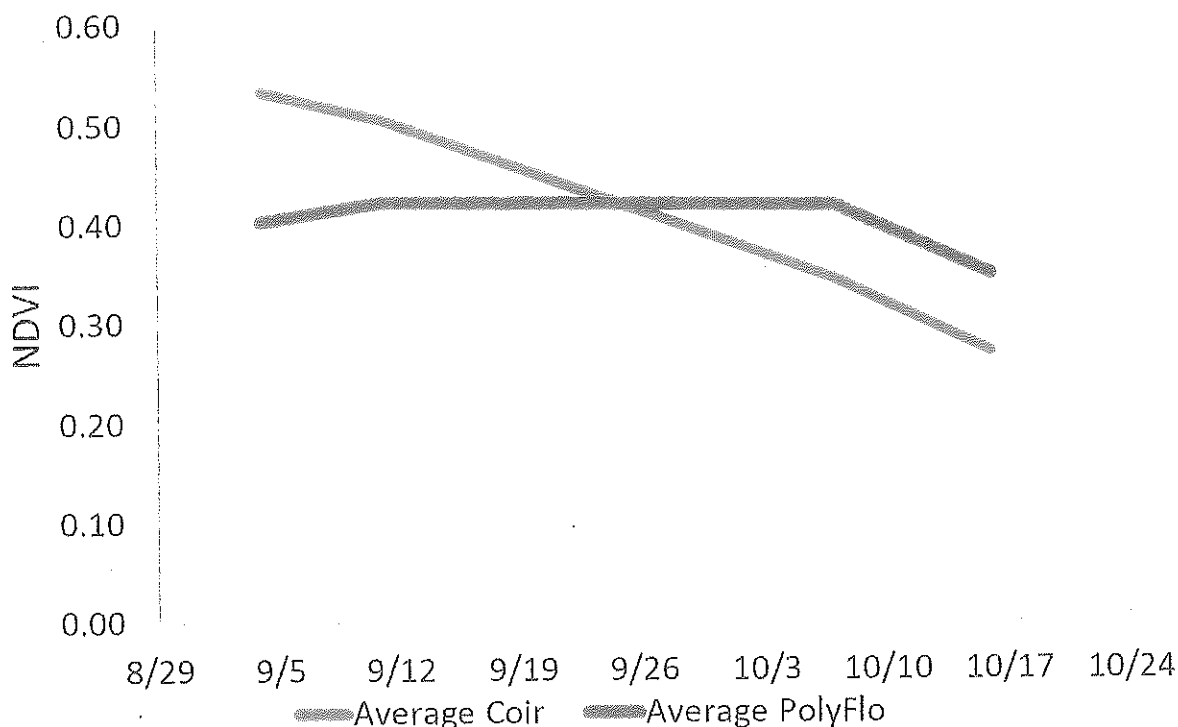


Figure 29. Average Greenseeker normalized difference vegetation index (NDVI) values measured at a constant height above floating wetland breakwater frames in September and October 2020.

4.6 Cost Analysis Comparison to Other Best Management Practices

BMPs that have traditionally been utilized to stop shoreline erosion include rip rap, retaining walls, and living shorelines. Biohaven has also developed a floating wetland breakwater with a median k_t of approximately 0.25 (Webb, 2014). Utilizing approximate material costs for each of these materials, in addition to the results from this study, we have compare the one-time materials cost and cost per day for no erosion for each of these BMPs (Table 13). The results show that the floating wetland breakwaters compare favorably with all these BMPs, while also providing additional ecosystem services compared to rip rap and retaining walls, and providing 18% more no-erosion days compared to Biohaven.

Table 13. Comparison of one-time materials cost and cost per day for no erosion over an assumed 20-year design life for various best management practices. These calculations do not consider inflation.

Best Management Practice	Material Cost per 10 ft section	Cost per Day of No Erosion over 20-yr Design Life *** (\$/day/ft)
Rip Rap	\$1,000-\$22,000	\$0.013-0.30
Retaining Walls	\$3,800-\$17,000	\$0.052-0.23
Living Shoreline	\$1,000-\$5,000	Not Determined
Biohaven Floating Wetland Breakwater	\$2,700	\$0.047 (78% of the days; estimated from the median k_t of 0.25 in Webb, 2014)
Floating Wetland Breakwater [11 pipes, 3 feet]	\$3,200	\$0.046 (96% of the days), not including shoreline plant growth benefits which would also decrease shoreline erodibility

Rip-rap Cost: various internet sources

Living Shorelines Cost Source: <https://www.fisheries.noaa.gov/insight/understanding-living-shorelines> ; reduction of erosion days cannot be estimated

Concrete Walls Cost Source: <http://southatlanticalliance.org/wp-content/uploads/2016/04/17-Hoffman-The-Costs-of-Shoreline-Stabilization.pdf>

Biohaven FWB Cost Source: Company quote; Percent wave reduction calculated based on Webb, 2014

** NOTE: Preliminary estimation that does not include installation, maintenance or time value of money; FWB costs should be reduced significantly with roto-mold

5 Lessons Learned and Design Alterations

Utilizing floating wetlands as a wavebreak in freshwater reservoirs is an innovative concept, and as a result, throughout the implementation process, many lessons have been learned. Unexpectedly, 2019 turned into a year of mostly trial and error with the floating wetland breakwaters, due to a period of much greater rainfall than is typical for the area in the week immediately following installation. Specifically, the Oklahoma Mesonet station in Norman received 11.34 inches of rainfall in April 2019, while the previous two years received 4.18 and 2.05 inches, respectively. These rain events caused Lake Thunderbird to rise approximately six feet according to COMCD, significantly higher than normal water level in the reservoir and inundated the floating wetlands. As a result, design modifications were made for the 2020 implementation to allow the floating wetlands to function more efficiently. These changes included (1) changes to the planting media design, (2) comparison of coir and Polyflo media during the 2020 implementation, and (3) adding cross supports to the frames for better initial support of the media and plants.

Changes to the plant media design were also made to increase their stability in the frames and provide additional protection for juvenile plants. To increase the stability of the Polyflo in the FWBs, which is a biological filter media designed to have high surface area for beneficial bacteria colonization as well as being durable and UV resistant, safety netting was wrapped around the plant media to create a “burrito” like system. The safety netting was then fastened to the frames themselves, allowing the plant media to be suspended within the FWBs. Figure 30 contains an example of one of the design modifications made to increase their stability in the FWB media.

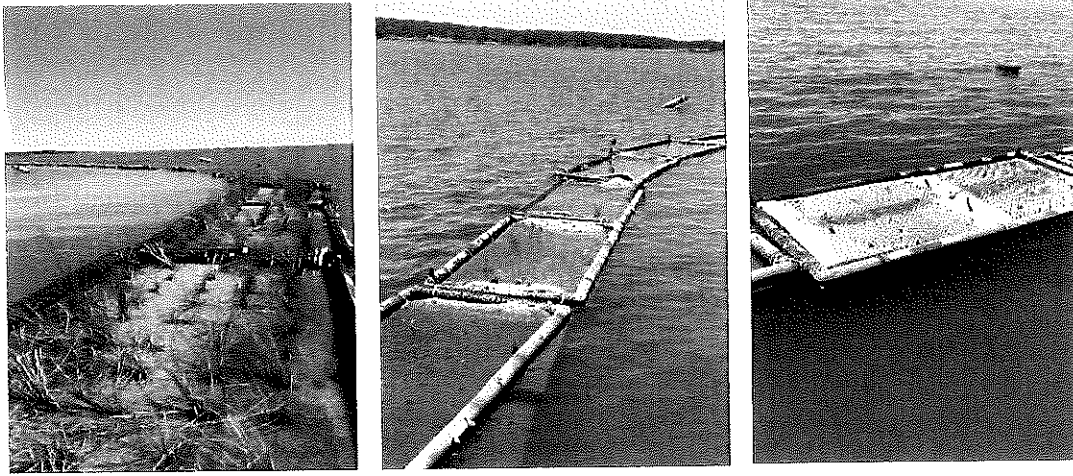


Figure 30. Evolution of floating wetland media design from initial planting and installation (left) to the damaged wetland frames (center), to finally the design modifications (right) to make the Polyflo more stable in the frames.

In addition to the Polyflo modifications, 10 of the 20 frames were outfitted with coir mattresses for the plant media in 2020 so that we could compare the coir mattresses to the PolyFlo burrito media. Coir is natural coconut fiber typically extracted from the outer husk of a coconut. Coir mattresses been implemented successfully in wetland restoration projects (Steve Patterson, personal communication). Figure 31 shows the process of creating the coir mattresses from shredding the coir bails to stitching the mattress together. These coir mattresses were then positioned, fastened, and planted in the FWB frames. Figure 32 shows the process of getting the mattresses situated in the frames and final attachment to the frames. As previously described, the Polyflo ultimately performed better at keeping plants alive (with our limited, opportunistic data collection).



Figure 31. Coir mattress production process.

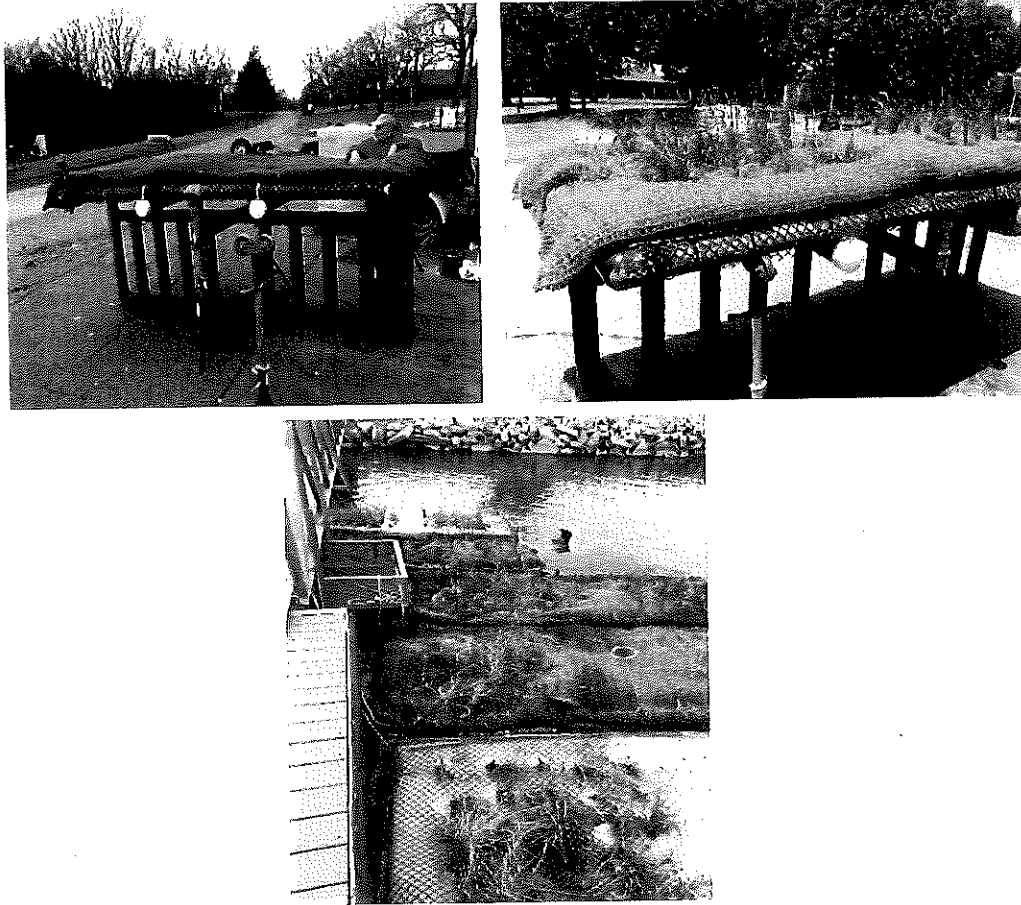


Figure 32. Demonstration of situating and planting the coir mattresses in the frame (top row), along with the frames positioned in the water (bottom image). Photos taken by Maxwell O'Brien.

Along with the new plant media design considerations, cross-support pipes were added to the floating frames themselves to provide additional structure for the plant media. The decision to add the cross supports was made because the original design did not keep the plant media structure high enough out of the water when water levels rose after planting, and resulted in the loss of the original plants along with the damage depicted in Figure 30 (center). Figure 33 shows a schematic that highlights the cross braces that were added to the original frame design. The cross braces were constructed using polyethylene pipe from the original frame construction process. The braces were filled with insulating spray foam sealant and then capped with PVC

caps prior to being fitted to the original FWB frames. It is important to note that these cross braces were added to the original design solely for the purpose of supporting the plant media and not to provide any additional wave break potential.

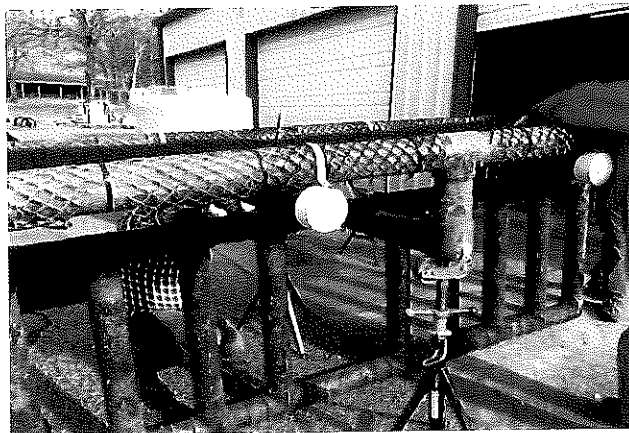
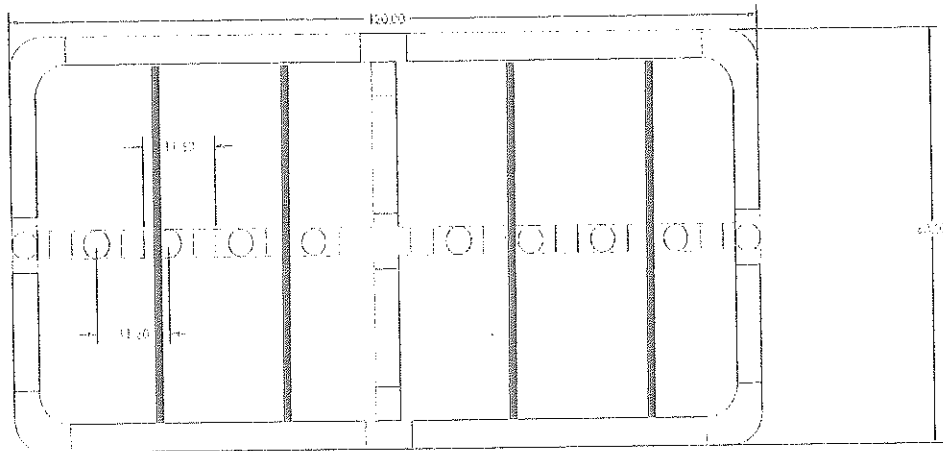


Figure 33. Top view (top) of the cross-brace modifications (blue) made to the original floating wetland breakwater design. Cross braces seen being attached to the floating wetland breakwater frame in the bottom image. Photo taken by Maxwell O'Brien.

6 Recommendations for Future Work

6.1 Media and Plant Establishment

While the primary objective of this study was to quantify and optimize the wave height and energy reduction potential of these systems, we also collected opportunistic measurements regarding plant establishment to best allow the FWBs also function as your traditional floating

wetland habitat. Throughout this study, whether it was from planting delays caused by procurement issues (2019) and COVID-19 halt to research (2020), extreme weather conditions, plant media damage, or vandalism, maintaining a thriving plant community on the FWBs was challenging. The modified frame and media design in 2020 that included the PolyFlo media and reworked frame and media design appeared to give the plants more support and they survived better. Along with the extra support, the planted frames were tethered around the boathouse at COMCD for approximately two weeks in spring 2020 to allow the aquatic vegetation to partially mature in the plant media. Prior to repositioning the frames back at their location out in the reservoir we noted what appeared to be healthy plants with roots growing through the plant media and into the water column seen in Figure 34. However, once the frames were repositioned out in the lake and the plants were exposed to all the conditions including wind, boat traffic, and even the reservoir freezing over, the plants on the frames did not have the opportunity to fully establish. For future deployment of FWBs, it is recommended to allow the plants to fully mature in their respective frames in a cove or other protected area, potentially for a full season, before moving them to a location with high wind speeds and wave action.



Figure 34. Roots from Juncus Effusus growing through PolyFlo media prior to field deployment in 2020.

6.2 One-piece Frame

The FWB frames used in the field portion of this project were constructed of PVC pipe that was welded together at each joint. After construction, each frame was towed into place behind the boat from the boat dock to the installation location. During this process, but unknown to us at that time, it appears that small leaks were caused in the joints at the locations of the PVC welds that were caused by the force of the water on the ballast pipes as it was towed through the water. This caused some of the frames to sit lower in the water than expected, which was then exacerbated by the extremely high water that occurred within a week of installation. To fix this issue, the research team proposes to utilize rotation molding for frame construction in the future. Rotational molding involves a heated hollow mold a charge of shot weight of material and then slowly rotated. This causes the softened material to disperse and stick to the walls of the mold, creating a one-piece plastic mold in the desired shape (source:

https://en.wikipedia.org/wiki/Rotational_molding). This will allow for increased ease and speed of transport of the frames from one location to the other.

6.3 Wave Measurement

During the project, multiple techniques for measure wave heights were utilized ranging from technical and complex (using an ADCP specifically designed to measure ocean waves) to simple (manually measuring wave height from GoPro video of the waves passing by a staff gage). Each of the techniques had their pros and cons, but our experience was that the simplest method of using a GoPro video of the waves passing by the staff gage was the most reliable and efficient. In addition, the ADCP we utilized, which was the only one that could be afforded on our budget, was designed for ocean waves and had problems measuring the height of small waves such as was found on the backside of the FWBs (this was not known by the company when it was purchased).

7 Summary and Conclusions

This project was able to meet all of its objectives and has advanced the understanding of utilizing FWBs to reduce shoreline erosion. Investigations at three scales—full-scale controlled mesocosm, laboratory-scale controlled mesocosm, and field scale, were completed. Through the full-scale controlled mesocosm study at the ARF on the University of Oklahoma campus, we demonstrated that a floating wetland frame with 11 pipe ballasts that were each 3-ft long for every ten feet of length provided the most cost-efficient wave energy reduction amongst the designs that were investigated. Furthermore, a companion laboratory-scale investigation concluded that, generally, FWB performance could be predicted utilizing scale models as long as similitude relationships were accounted for (especially force similitude, which is the hardest to achieve on scale models). The field implementation in Lake Thunderbird proved to have the best

reported, consistent wave reduction not only amongst our designs, but also compared to available transmission coefficients reported in available literature for other breakwater designs. Additionally, the materials cost was shown to be competitive related to other traditional and bio-engineered practices for reducing shoreline erosion.

As part of the research project we were able to identify design improvements that can be implemented going forward including (1) utilizing PolyFlo media with cross braces for the best integrity of the media in the FWBs; (2) if possible establish the plants in a cove or other protected area for one growing season before implementing in a location with large waves; (3) a rotational mold of the FWB frame would be useful so that there are not seams that can leak on the frame; and, (4) if monitoring is required, simple manual measurements using a GoPro and and stage gage may be the most efficient and reliable mode of measuring wave heights and periods.

This of innovative concept of utilizing FWB with ballasts to optimize wave reduction and reduce shoreline erosion design has shown promise to simultaneously function as a floating wetland and a wave break. Our team sees this design as a cost-effective alternative for reducing shoreline erosion in areas with moderate erosion, which will allow nature time to heal the shoreline before moving the system to the next location.

References

- Allen, H., (2001 Dec 27), Shoreline Erosion Control Plan, Lake Thunderbird, AllEnVironment Consulting, Vicksburg, MS.
- Bengtsson, Lars, and Thomas Hellström. "Wild-induced resuspension in a small shallow lake." *Hydrobiologia* 241.3 (1992): 163-172.
- Claussen, J. E. (2015). "Largemouth Bass *Micropterus salmoides* (Lacepède, 1802)." <https://scholar.google.com/citations?view_op=view_citation&hl=en&user=G9K35TQAAAAJ&citation_for_view=G9K35TQAAAAJ:YFjsv_pBGBYC> (Aug. 5, 2021).

- Coops, Hugo, Noël Geilen, Henk J. Verheij, René Boeters, and Gerard van der Velde. (1996) "Interactions between waves, bank erosion and emergent vegetation: an experimental study in a wave tank." *Aquatic Botany* 53, no. 3-4 (1996): 187-198.
- Deigaard, Rolf, and Jørgen Fredsøe. "Shear stress distribution in dissipative water waves." *Coastal Engineering* 13.4 (1989): 357-378.
- Denny, M. W. (1995). Predicting physical disturbance: Mechanistic approaches to the study of survivorship on wave-swept shores. *Ecol. Monogr.* 65, 371–418.
- Denny, Mark, and Brian Gaylord. "The mechanics of wave-swept algae." *Journal of Experimental Biology* 205.10 (2002): 1355-1362.
- Environmental Protection Agency. (2006) The rock manual: The use of rock in hydraulic engineering (2nd edition). Retrieved October 07, 2020.
- Garcia Chance LM, White SA. 2018. Aeration and plant coverage influence floating treatment wetland remediation efficacy. *Ecological Engineering*. 122:62–68. doi:10.1016/j.ecoleng.2018.07.011.
- Gatto, L. W. (1988). *Techniques for Measuring Reservoir Bank Erosion*. Cold Regions Research and Engineering Lab Hanover, NH.
- Hanson, G. J., and Cook, K. R. (2004). "Apparatus, test procedures, and analytical methods to measure soil erodibility in situ." *Applied Engineering in Agriculture*, 20.
- Harms, VW (1979). Floating breakwater performance comparison. Conference: 17. International Conference on Coastal Engineering, Sydney, Australia, 23 Mar 1980.
- Headley, T. R., and Tanner, C. C. (2008). "Floating Treatment Wetlands: an Innovative Option for Stormwater Quality Applications." 6.
- Hochstein, Anatoly B, and Adams, Jr, Charles E. A Numerical Model of the Effects of Propeller Wash and Ship-Induced Waves from Commercial Navigation in an Extended Navigation Season on Erosion, Sedimentation, and Water Quality in the Great Lakes Connecting Channels and Harbors, 1986.
- Kamphuis, J. William, and Kevin R. Hall. "Cohesive material erosion by unidirectional current." *Journal of Hydraulic Engineering* 109.1 (1983): 49-61.
- Kinsman, B., 2002. Wind Waves: Their Generation and Propagation on the Ocean Surface. United States of America: Dover Publications.
- Klavon, K., Fox, G., Guertault, L., Langendoen, E., Enlow, H., Miller, R., and Khanal, A. (2017). "Evaluating a process-based model for use in streambank stabilization: insights on the Bank Stability and Toe Erosion Model (BSTEM)." *Earth Surface Processes and Landforms*, 42(1), 191–213.
- Leonardi, N., Ganju, N., & Fagherazzi, S. (2016). A linear relationship between wave power and erosion determines salt-marsh resilience to violent storms and hurricanes. *Proceedings of the National Academy of Sciences of the United States of America*, 113(1), 64-68. Retrieved October 7, 2020.
- Marani, M., D'Alpaos, A., Lanzoni, S., & Santalucia, M. (2011). Understanding and predicting wave erosion of marsh edges. *Geophysical Research Letters*, 38(21)
- Martin Ecosystems., 2017 Jul 12, BioHaven Floating Wetland Technology White Paper, Martin Ecosystems.

- Mehaute, B. L. (1976). *An Introduction to Hydrodynamics and Water Waves*. Springer Study Edition, Springer-Verlag, Berlin Heidelberg.
- Miller, R. R. (1960). Systematics and biology of the gizzard shad (*Dorosoma cepedianum*) and related fishes. *Fisheries*, 1(2), 3.
- National Geographic Society, 2018. Erosion, [accessed 2019 Feb 22].
<http://www.nationalgeographic.org/encyclopedia/erosion/http://www.nationalgeographic.org/encyclopedia/erosion/>.
- Neelamani, S, and Ljubic, Josko. "Experimental Study on the Hydrodynamic Performance of Floating Pontoon Type Breakwater With Skirt Walls." *Journal of Offshore Mechanics and Arctic Engineering*, vol. 140, no. 2, 2018, pp. *Journal of offshore mechanics and Arctic engineering*, 2018-04-01, Vol.140 (2).
- Oklahoma Department of Environmental Quality (ODEQ), 2020. Water Quality in Oklahoma, 2020 Integrated Report. Source: <https://www.deq.ok.gov/water-quality-division/watershed-planning/integrated-report/>
- Oklahoma Water Resources Board. (2002). "Lake Thunderbird Capacity and Water Quality 2001." *Final*
- Ozeren, Y., & Wren, D. (2018). Wave Erosion of Cohesive and non-Cohesive Embankments: Laboratory Experiments. Retrieved October 7, 2020.
- Ozeren, Yavuz. "Experimental and Numerical Investigations of Floating Breakwater Performance." The University of Mississippi, ProQuest Dissertations Publishing, 2009.
- Sadeghian, Amir, et al. "Sedimentation and Erosion in Lake Diefenbaker, Canada: Solutions for Shoreline Retreat Monitoring." *Environmental Monitoring and Assessment*, vol. 189, no. 10, 2017, p. 507.
- Sayah et al., 2005, Field Measurements and Numerical Modelling of Wind-Waves in Lake Biel: A Basic Tool for Shore Protection Projects, Proceedings of the XXXI IAHR Congress, Seoul, Korea, 4332-4343.
- Smyth, C., and Alex E. Hay. "Wave friction factors in nearshore sands." *Journal of Physical Oceanography* 32.12 (2002): 3490-3498.
- Stern, F. (2013). Chapter 7 Dimensional Analysis and Modeling. Retrieved 2020.
- Stewart, F. M., Muholland, T., Cunningham, A. B., Kania, B. G., and Osterlund, M. T. (2008). "Floating islands as an alternative to constructed wetlands for treatment of excess nutrients from agricultural and municipal wastes – results of laboratory-scale tests." *Land Contamination & Reclamation*, 16(1), 25–33.
- Strosnider, W., Schultz, S., Strosnider, K., and Nairn, R. (2017). "Effects on the Underlying Water Column by Extensive Floating Treatment Wetlands." *Journal of Environment Quality*, 46, 201.
- Thurman, H. V., & Trujillo, A. P. (2001). *Essentials of oceanography*. Englewood Cliffs, N.J.: Prentice Hall.
- Uzaki, K., Ikehata, Y., and Matsunaga, N. (2011, July 1–October 11). Performance of the wave energy dissipation of a floating breakwater with truss structures and the quantification of transmission coefficients. Retrieved October 07, 2020.
- Webb, Brett M., 2014 Mar 14, Wave transmission testing of the Martin Ecosystems BioHaven Floating Breakwater, Department of Civil Engineering, University of Alabama.